Chapter 15
Purification of Toxic Compounds in Water and Treatment of Polymeric Materials

Ho-In Lee, Jae-Hyun Kim, Han-Su Lee, and Weon-Doo Lee

Abstract Among a variety of semiconductors as the medium for photocatalytic treatment of pollutants in the form of suspended powders or immobilized phases, titanium dioxide is the most widely used due to its high stability, good performance, and low cost. In this chapter, photocatalysis of aqueous pollutants covers both organic pollutants, including pyrimidines, phenols, pesticides, synthetic dyes, etc., and inorganic pollutants, mainly focusing on nitrogen-containing ones. In the latter section, application to polymer science encircles applications to pigmentation, photocatalyst–polymer composites, and functional coating.

1 Introduction

Since Fujishima and Honda (1972) discovered the photocatalytic splitting of water on TiO_2 electrodes under UV illumination, photocatalysis has been widely applied in solar energy conversion, air and wastewater treatment, sterilization, induction of super-hydrophilicity, cancer treatment, etc.

Excitation of semiconductor materials such as TiO_2 with light of wavelength shorter than the bandgap cutoff wavelength results in the formation of electron–hole pairs. The photogenerated electron–hole pairs experience a series of events as below (Serpone and Khairutdinov 1997).

Charge-carrier migration to surface:

$$e^-_{CB} \rightarrow e^-_s \tag{1}$$

H.-I. Lee (✉)
School of Chemical and Biological Engineering, Seoul National University, Seoul 151-744, Korea
e-mail: hilee@snu.ac.kr

M. Anpo and P.V. Kamat (eds.), *Environmentally Benign Photocatalysts*, Nanostructure Science and Technology, DOI 10.1007/978-0-387-48444-0_15,

$$h^+_{VB} \rightarrow h^+_s \tag{2}$$

Charge-carrier trapping into shallow traps (ST):

$$e^-_{CB} + (ST)_e \rightarrow e^-_{ST} \tag{3}$$

$$h^+_{VB} + (ST)_h \rightarrow h^+_{ST} \tag{4}$$

$$e^-_{CB} + Ti^{4+} \rightarrow Ti^{3+} \tag{5}$$

$$h^+_{CB} + {>}Ti^{4+} - OH \rightarrow {>}Ti^{4+} - {}^{\bullet}OH \tag{6}$$

Charge-carrier recombination:

$$e^-_{CB} + h^+_{VB} \rightarrow h\nu_1 \tag{7}$$

$$e^-_{ST} + h^+_{VB} \rightarrow h\nu_2 \tag{8}$$

$$e^-_{CB} + h^+_{ST} \rightarrow h\nu_3 \tag{9}$$

$$e^-_{ST} + h^+_{ST} \rightarrow h\nu_4 \tag{10}$$

$${>}Ti^{4+} - {}^{\bullet}OH + Ti^{3+} \rightarrow h\nu_5 \tag{11}$$

Hole or electron trapping by shallow traps such as bulk defects triggers charge-carrier recombination and reduces the efficiency of photocatalysis. The holes that reach the surface and are trapped by surface defects or surface hydroxyl groups can cause photocatalytic oxidation. Simultaneously, surface electrons are able to cause photocatalytic reduction. When photocatalysis is applied to oxidation, a sacrificial electron acceptor must be used. On the contrary, an application to photocatalytic reduction requires a hole scavenger (Lee et al. 2001a).

Although the majority of photocatalytic organic pollutant treatments progress via oxidation mechanism, photocatalytic reduction also enables many useful reactions to occur. For example, hydrogen evolution, metal ion recovery, nitrogen fixation, CO_2 fixation, etc., take place via photocatalytic reduction (Lee and Lee 1998; Lee et al. 2001b).

2 Mechanistic Approach

Photocatalytic processes make use of semiconductor metal oxide as a catalyst and oxygen as an oxidizing agent. Many catalysts have been tested so far, although only TiO_2 in the anatase form seems to have functional attributes such as high stability,

good performance, low cost, and easy separation/regeneration after processes (Lee et al. 2001c). It is no surprise that different samples of TiO_2 exhibit different photocatalytic activities toward same organic substrates under otherwise identical reaction conditions. Such differences can be qualitatively attributed to differences in morphology, crystal phase, specific surface area, particle aggregate size, and surface density of OH groups in the TiO_2 samples.

Bhatkhande et al. (2001) summarized the types of organic and inorganic substances that can be degraded using photocatalysis. Almost all kinds of substances can be treated and lists of these substances are also found in other review papers (Agustina et al. 2005; Carp et al. 2004; Gogate and Pandit 2004; Diebold 2003; Pirkanniemi and Sillanpää 2002; Blake 2001; Herrmann 1999; Mills and Le Hunte 1997; Jung and Lee 1997; Hoffmann et al. 1995; Lee and Lee 1992).

The photocatalytic oxidation of organic pollutants can progress via two mechanisms: "indirect oxidation" and "direct oxidation" (Serpone et al. 1995). In the first "indirect oxidation" mechanism, photogenerated valence holes react primarily with physisorbed H_2O and surface-bound hydroxyl groups (–OH) on TiO_2 particles to give OH radicals that may then react with organic molecules. Typically, the mechanism of OH radical formation has been presumed as follows (Wang et al. 1999; Hirakawa and Nokada 2002).

$$H_2O + h_s^+ \rightarrow {}^\bullet OH + H^+ \tag{12}$$

$$OH_s^- + h_s^+ \rightarrow {}^\bullet OH \tag{13}$$

$$O_2 + e_s^- \rightarrow {}^\bullet O_2{}^- \tag{14}$$

$${}^\bullet O_2{}^- + H^+ \leftrightarrow {}^\bullet HO_2 \tag{15}$$

$${}^\bullet HO_2 + {}^\bullet HO_2 \rightarrow H_2O_2 + O_2 \tag{16}$$

$${}^\bullet O_2{}^- + {}^\bullet HO_2 \rightarrow HO_2{}^- + O_2 \tag{17}$$

$$HO_2{}^- + H^+ \rightarrow H_2O_2 \tag{18}$$

$$H_2O_2 + {}^\bullet O_2{}^- \rightarrow {}^\bullet OH + OH^- + O_2 \tag{19}$$

$$H_2O_2 + h\nu \rightarrow 2{}^\bullet OH \tag{20}$$

Turchi and Ollis (1990) proposed that the average diffusion distance of OH radicals could be extended to 10^{-6} m in slurry reactors. Therefore, the interaction of organic molecules with OH radicals is possible at solution bulk. In the second "direct oxidation" mechanism, the valence band holes directly react with organic substrates.

Following the formation of active species such as photogenerated holes and OH radicals explained above, the overall processes can be divided into five independent steps (Herrmann 1999):

1. Transfer of reactants in the fluid phase to the surface
2. Adsorption of at least one of the reactants
3. Reaction in the adsorbed phase
4. Desorption of products
5. Removal of the products from the interface region

Based on the above processes, Langmuir–Hinshelwood kinetic model could be applied to the reaction occurring at the solid–liquid interface (Fox and Duray 1993)

$$r_{\mathrm{LH}} = -\frac{\mathrm{d}C}{\mathrm{d}t} = k\theta = \frac{kKC}{1+KC}, \tag{21}$$

where C, k, and K, respectively, represent the concentration of the organic compound to be decomposed, the reaction rate constant, and the equilibrium adsorption coefficient.

For diluted solutions ($C < 10^{-3}$ M), KC becomes $\ll 1$ and the reaction is of the apparent first order, whereas for $C > 5 \times 10^{-3}$ M, ($KC \gg 1$), the reaction rate is maximum and of the zero order. This Langmuir–Hinshelwood kinetics has been widely used for the understanding of photocatalytic oxidation mechanism.

The oxidative ability of photocatalyst has been largely applied to the decomposition of various volatile organic compounds or aqueous organic pollutants (Herrmann 1999; Mills and Le Hunte 1997; Fox and Duray 1993). Nearly all of the organic pollutants can be totally mineralized to CO_2 by photocatalysis with the exception of *s*-triazine herbicides of which the final products are cyanuric acids. Photocatalysis and biodegradation must be combined for total mineralization of cyanuric acids and *s*-triazine ring compounds. Chlorinated organic compounds, organic nitrogen compounds, organic sulfur compounds, and organic phosphorous compounds are mineralized to release chlorine ions, ammonium and/or nitrate ions, sulfate ions, and phosphate ions, respectively (Halmann 1996). Recently, various commercial processes are adapted to wastewater treatment (see Fig. 1 from http://purifics.com/products/photo-cat.html).

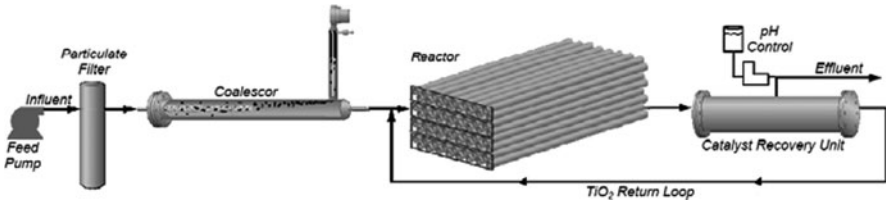

Fig. 1 Commercial photocatalytic wastewater process

2.1 Mechanistic Models

The main pathway of photomineralization (i.e., the breakdown of organic compounds) carried out in aerated solution may easily be summarized by the following reaction:

$$\text{Organic compounds} \rightarrow CO_2 + H_2O + \text{mineral acids} \tag{22}$$

A schematic representation of this process is displayed in Fig. 2 (Carp et al. 2004).

The radical ions formed after the interfacial charge transfer reactions can participate in several pathways of the degradation process:

1. They may react chemically with themselves or with surface-adsorbed compounds.
2. They may recombine via back electron-transfer reactions, especially when they are trapped near the surface, due to either the slowed-down outward diffusion or hydrophobicity.
3. They may diffuse from the semiconductor surface and participate in chemical reactions in the bulk solution.

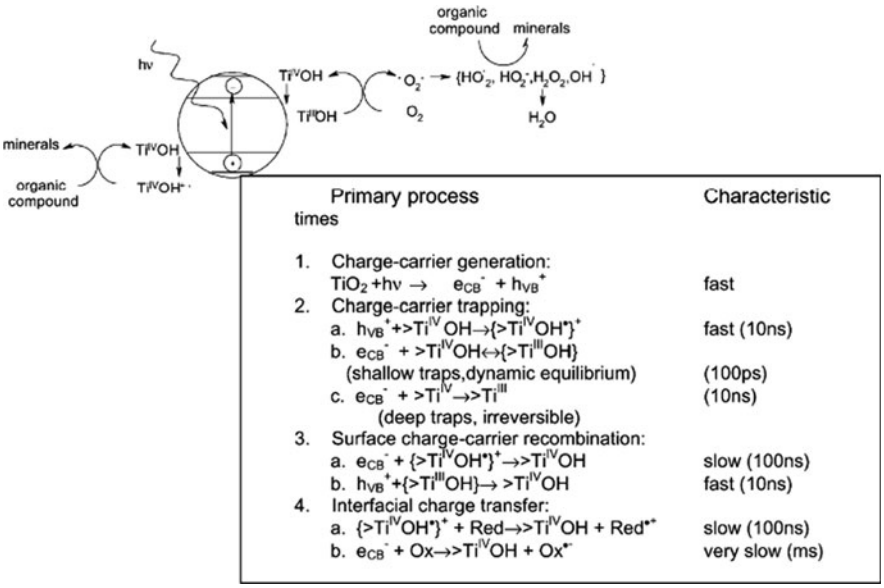

Fig. 2 Major processes and their characteristic times for TiO_2-sensitized photo-oxidative mineralization of organic compounds by dissolved oxygen in aqueous solutions. Reprinted from Carp et al. (2004), Copyright with permission from Elsevier

Detailed mechanism of the photocatalytic process on TiO_2 surface is still not completely clear, particularly that of the initial steps involved in the reaction of reactive oxygen species and organic molecules.

A reasonable assumption is that both photocatalytic oxidative and reductive reactions occur simultaneously on the TiO_2 particle, since charge would build up otherwise. In most experiments, the electron transfer to oxygen, which acts as a primary electron acceptor, is rate-determining in photocatalysis. Hydroxyl radicals are formed on the surface of TiO_2 by reaction of holes in the valence band (h^+_{vb}) with adsorbed H_2O, hydroxide, or surface titanol groups (>TiOH). The photogenerated electrons are reduced enough to produce superoxide (O_2^-). This superoxide is an effective oxygenation agent that attacks neutral substrates as well as surface-adsorbed radicals and/or radical ions. Theoretically, the redox potential of the electron–hole pair permits H_2O_2 formation either by water oxidation (by holes) or by two conduction band electron reduction of the adsorbed oxygen. The latter represents the main pathway of H_2O_2 formation. H_2O_2 contributes to the degradation pathway by acting as an electron acceptor or as a direct source of hydroxyl radicals subsequent to homolytic scission. Depending on the reaction conditions, the holes, •OH radicals, O_2^-, H_2O_2, and O_2 can play important roles in the photocatalytical reaction mechanism. These processes are presented in Fig. 3 (Hoffmann et al. 1995). If non-oxygenated products, derived from ion radicals, are desired, oxygen has to be replaced with other electron acceptors.

According to the above-mentioned mechanism and time characteristics, two critical processes determine the overall quantum efficiency of interfacial charge transfer:

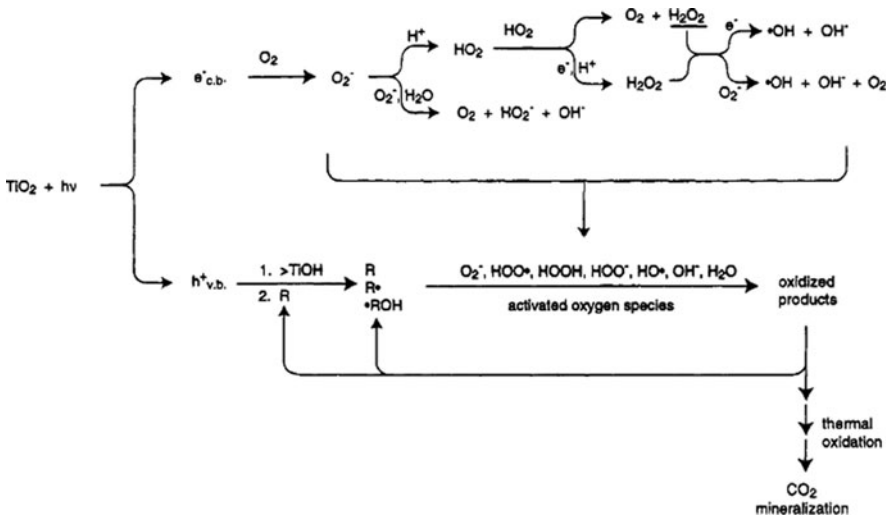

Fig. 3 Secondary reactions with activated oxygen species in the photoelectron-chemical mechanism. Reprinted with permission from Hoffmann et al. (1995), Copyright, American Chemical Society

1. Competition between charge-carrier recombination and trapping (picoseconds to nanoseconds)
2. Competition between trapped carrier recombination and interfacial charge transfer (microseconds to milliseconds)

An increase in either charge-carrier lifetime or the interfacial electron-transfer rate is expected to lead to higher quantum efficiency for steady state photolysis.

2.2 Operational Parameters

It has been demonstrated that catalyst dosage, character and initial concentration of the target compound, coexisting compounds, UV light intensity, oxygen concentration, presence of supplementary oxidizable substances, temperature, circulating flow rate, pH for aqueous treatments, and water concentration for gaseous phase photoreactions are the main parameters affecting the degradation rate. Each of these parameters will be discussed in the following section (Carp et al. 2004; Gogate and Pandit 2004; Herrmann 1995).

Generally, decomposition rate increases with catalyst loading due to higher surface area of the catalyst that is available for adsorption and degradation. An optimum value is present, while above a certain concentration, the solution opacity increases (due to increased light scattering of the catalyst particles), causing a reduction in light penetration through the solution and a consequent rate decrease. Additionally, at high-TiO_2 concentrations, terminal reaction (23) could also contribute to the diminution of photodegradation rate. The formed hydroperoxyl radical is less reactive than the HO• one:

$$H_2O_2 + HO^{\bullet} \rightarrow H_2O + HO_2^{\bullet} \tag{23}$$

The optimal catalyst dosage or effective optical penetration length, under given conditions, is very important in designing a slurry reactor that makes effective use of the reactor space and the catalyst. If the solution layer thickness exceeds the optical penetration length at any given illumination intensity and catalyst concentration, the photoreactor will be under-utilized.

For TiO_2 immobilized systems, there is also an optimal thickness of the catalyst film. The interfacial area is proportional to the thickness of catalyst, as the film is porous. Thus, thick films favor catalytic oxidation. On the other hand, the internal mass transfer resistance for both organic species and photogenerated electrons/holes increases with increasing thickness. This increases the recombination possibility of the electron/hole pair and as a consequence, the degradation performance is reduced.

Usually reactor designs should be such that uniform irradiation of the entire catalyst surface is achieved at the incident light intensity. This is a major problem associated with the large-scale designs. Moreover, nearly complete elimination of mass transfer resistances is another point that needs to be considered while

designing large-scale reactors. The efficient reactor design must expose highest amount of the activated immobilized catalyst to the illuminated surface and must have a high density of active catalyst in contact with the liquid to be treated inside the reactor.

The degradation rate of organic substrates usually exhibits saturation behavior: the observed rate constant decreases with an increase in the initial organic pollutant concentration. Three factors may be responsible for this behavior:

1. The main steps in the photocatalytic process occur on the surface of the solid photocatalyst. Therefore, a high adsorption capacity is reaction favoring. Because most of the reactions follow an LH equation, this means that at a high initial concentration all catalytic sites are occupied. A further increase in the concentration does not affect the actual catalyst surface concentration and, therefore, may result in a decrease of the observed first-order rate constant.
2. The generation and migration of photogenerated electron–hole pairs and their reaction with organic compounds occur in series. Therefore, each step may become rate-determining for the overall process. At low concentrations, the latter dominates the process and, therefore, the degradation rate increases linearly with concentration. However, at high concentrations, the former will become the governing step and the degradation rate increases slowly with concentration. For a given illumination intensity, even a constant degradation rate may be observed as a function of concentration.
3. Intermediates generated during the photocatalytic process also affect the rate constant of their parent compounds. A higher initial concentration will yield a higher concentration of adsorbed intermediates, which will affect the overall rate.

It is well known that the photocatalytic oxidation rate is not affected much by minor changes in temperature. This weak dependence is reflected by the low activation energy of photocatalytic oxidation reactions (a few kJ/mol) compared to ordinary thermal reactions. This is due to the low thermal energy ($kT = 0.026$ eV at room temperature) that has almost no contribution to the activation energy of (the wide bandgap) TiO_2. On the other hand, these activation energies are quite close to that of hydroxyl radical formation, suggesting that the photodegradation of these organics is governed by hydroxyl radical reactions (Matthews 1987). The effect of temperature on the rate of oxidation may be dominated by the rate of interfacial electron transfer to oxygen (Anpo et al. 1987). Alternatively, the more rapid desorption of both substrates and intermediates from the catalyst at higher temperatures is probably an additional factor, leading to a larger effective surface area for the reaction. At lower temperatures, desorption becomes the rate-limiting step of the process (Herrmann 1999).

Even though changes in relative positions of the Fermi level of TiO_2 powders at temperatures between 21 and 75°C have been reported as relatively small (0.04 eV), improved interfacial electron-transfer kinetics are observed when the temperature is increased (Kiwi 1985). In the range of 20–80°C, weak dependence of degradation rates on temperature has usually been observed. As a consequence, the optimum temperature is generally comprised between 20 and 80°C.

There are two regimes of the photocatalytic reaction with respect to the UV-photon flux. They comprise a first-order regime for fluxes up to about 25 mW/cm^2 in laboratory experiments and a half-order regime for higher intensities. In the former regime, the electron–hole pairs are consumed more rapidly by chemical reactions than by recombination reactions, whereas in the half-order regime, the recombination rate is dominant (Herrmann 1995). The variation of reaction rate as a function of the wavelength used follows the adsorption spectrum of the catalyst with a threshold corresponding to its band energy.

Oxygen was found to be essential for semiconductor photocatalytic degradation of organic compounds. Dissolved molecular oxygen is strongly electrophilic and thus an increase of its content probably reduces unfavorable electron–hole recombination routes. But higher concentrations lead to a downturn in the reaction rate, which could be attributed to the fact that the TiO_2 surface becomes excessively hydroxylated to the extent of inhibiting the adsorption of pollutant at active sites.

The influence of oxygen pressure on the liquid phase is difficult to study because the reaction is polyphasic. Generally, it is assumed that O_2 adsorbs on TiO_2 from the liquid phase, where its concentration is proportional to the gas phase oxygen pressure according to Henry's law. Apart from its conventional electron scavenging function, the dissolved O_2 may play a key role in the degradation of organic compounds.

Medium pH has a complex effect on the rate of photocatalytic oxidation, and the observed effect is generally dependent on the type of the pollutant as well as the point of zero charge (pzc) of the semiconductor used in the oxidation process, i.e., more specifically on the electrostatic interaction between the catalyst surface and the pollutant. The adsorption of the pollutant and hence the degradation rate will be maximum near the pzc of the catalyst. For some of the pollutants that are weakly acidic, rate of photocatalytic oxidation increases at lower pH due to an increase in the extent of adsorption under acidic conditions. Some of the pollutants that undergo hydrolysis under alkaline conditions or undergo decomposition over a certain pH range may show an increase in the rate of photocatalytic oxidation with an increase in the pH. Since the effect of pH cannot be generalized, it is recommended that laboratory scale studies are required to establish the optimum conditions for the operating pH unless data are available in the literatures with identical operating conditions, i.e., the type of equipments as well as the range of operating parameters, including the composition of the effluent stream (Gogate and Pandit 2004).

Presence of ions may affect the degradation process via adsorption of contaminants; reaction with hydroxyl radical ions and/or absorption of UV light. This is a very important point that needs to be considered as real life industrial effluents will have different types of salts at different levels of concentration and generally these are in ionized forms. In general, it can be said that CO_3^{2-}, HCO_3^- (they act as radical scavengers and also affect the adsorption process), and Cl^- (affects the adsorption step strongly and also partly absorbs UV light) ions have strong detrimental effect on the degradation process whereas other anions such as sulfate, phosphate, and nitrate affect the degradation efficiency marginally.

$$h^+ + SO_4^{2-} \rightarrow SO_4^{\bullet -} \quad (24)$$

$$h^+ + H_2PO_4^{2-} \rightarrow H_2PO_4 \quad (25)$$

These radicals may initiate oxidation reactions with organic species. Yawalkar et al. (2001) have studied the effect of SO_4^{2-}, CO_3^{2-}, Cl^-, and HCO_3^- ions on the overall degradation rates of phenol and reported that the detrimental effects are observed in the order of $SO_4^{2-} < CO_3^{2-} < Cl^- < HCO_3^-$.

For cations, both beneficial and detrimental effects have been evidenced. The effect is strongly dependent on the metallic ion nature and their concentrations. The rate of photocatalytic degradation can be enhanced up to an optimum value. Metal ions may increase the photocatalytic rate due to:

1. The ability of metallic ions to trap either electrons or holes via oxidizing and reducing reactions
2. Alternative homogeneous Fenton-type reactions on the TiO_2 surface that lead to additional HO• production
3. Short-circuiting reactions that create a cyclic process without generation of active HO•
4. Filter effect due to UV absorption of the species
5. Precipitation and deposition of the dissolved metallic ions as hydroxides on the TiO_2 surface

Although photocatalysis has shown to be adequate for the destruction of a wide variety of compounds, in some cases the complete mineralization is slowly attained, and the efficiency of the processes, in terms of energy consumption, is only advantageous for very dilute effluents. To overcome this difficulty, some additives such as H_2O_2, Fe^{2+}, Fe^{3+}, $S_2O_8^{2-}$, Ag^+, etc., with different chemical roles can be added to the photocatalytic systems (Agustina et al. 2005).

Another drawback in photocatalytic degradation of wastewaters is the need for transparency of treated wastewater at the spectral region where semiconductor absorbs. Some ideas have been published to enable the use of photocatalysis even when the wastewater is not transparent enough. In multiple tube reactor with TiO_2-coated hollow glass tubes, UV-light travels through the inside of hollow tubes while wastewater flows over the outside of the tubes (Ray and Beenackers 1998). Somewhat similar idea is to embed TiO_2 onto glass fibers to increase the penetration of UV-light into the wastewater solution (Hofstadler et al. 1994).

3 Pyrimidine and Its Derivatives

Organic compounds containing nitrogen atoms are extremely common in nature. The prevalent category includes amino acids, proteins, and several classes of man-made substances of environmental concern that have nitrogen atoms in their structures, such

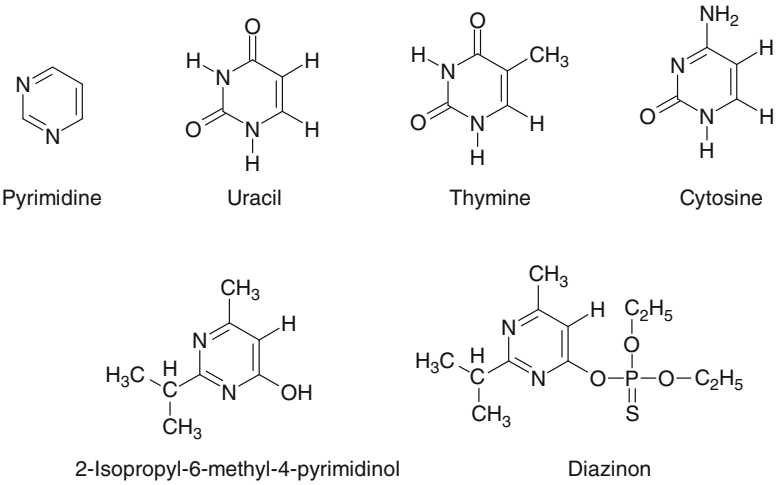

Fig. 4 Some examples of pyrimidine and its derivatives

as herbicides, pesticides, drugs, explosives, and dyes. Among organic nitrogen compounds, pyrimidine derivatives are mainly found in biomolecules and agrochemicals. Some examples of pyrimidine and its derivatives are shown in Fig. 4. There have been a few works about photocatalytic degradation of pyrimidine compounds. Major studies focused on the degradation mechanism of DNA bases (uracil, thymine, and cytosine) and the effect of coexistent ions on the activity of the photocatalyst (Dhananjeyan et al. 1996, 1997, 2000a, b; Horikoshi et al. 1999; Jaussaud et al. 2000; Horikoshi and Hidaka 2001; Calza et al. 2004). Several reports dealt with the photocatalytic degradation of pyrimidine derivative pesticides such as diazinon and 2-isopropyl-6-methyl-4-pyrimidinol (IMP) (Kouloumbos et al. 2003; Lee et al. 2003, 2004, 2005; Oh et al. 2006, 2007). These studies are reviewed in this chapter.

3.1 Oxidation Mechanism

It has been reported that pyrimidine glycols are found as reaction products, suggesting that photocatalytic oxidation of pyrimidine derivatives is progressed via indirect oxidation by hydroxyl radical (Dhananjeyan et al. 1996, 1997; Jaussaud et al. 2000). Hydroxylation of pyrimidine ring results in ring opening. The kinds and positions of functional groups, that cause differences in frontier electron density, determine the attack position of hydroxyl radical and chain cleavages leading to different degradation mechanisms and final products. In a decomposition case of pyrimidine molecules, C–N cleavage caused by hydroxyl radical gives birth to more NH_4^+ than NO_3^- (see Fig. 5) (Horikoshi and Hidaka 2001). The pyrimidine derivatives substituted by amino group, such as cytosine and 4-aminopyrimidine, also show similar results. However, the photocatalytic degradation of uracil and

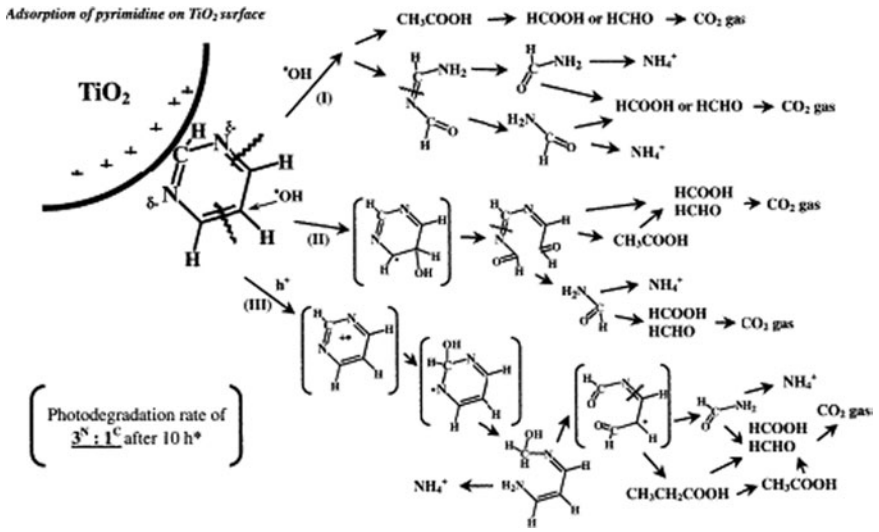

Fig. 5 Photodegradation mechanism of pyrimidine. Reprinted from Horikoshi and Hidaka (2001), Copyright with permission from Elsevier

thymine containing carboxyl groups produces more NO_3^- than NH_4^+, following primary amine formation (Horikoshi et al. 1999; Calza et al. 2004). When the amino group is positioned on carbon 2 in aminopyrimidine, guanidine is formed as a very stable intermediate, as opposed to the case of 4-aminopyrimidine (Calza et al. 2004).

Diazinon, an organophosphorous insecticide with widespread agricultural and non-agricultural uses, is also decomposed by hydroxyl radical and as IMP is produced (see Fig. 6) (Kouloumbos et al. 2003).

IMP is totally mineralized via ring-opening by photocatalytic oxidation. UV absorption spectrum changes of IMP during photocatalytic reaction are shown in Fig. 7. Two peaks that result from pyrimidine ring disappeared as the reaction progressed, suggesting that pyrimidine ring opening took place by photocatalytic reaction. Acetamide, a possible fragment of the IMP ring, was also detected in the GC-Mass analysis of reaction intermediates. The theoretical amount of CO_2 that could be evolved through the complete oxidation of IMP was estimated to be about 1,250 μmol. Also, the total evolved amount of CO_2 was 1,200 μmol, similar to the theoretical amount (Lee et al. 2003).

Photocatalytic oxidation steps of pyrimidine derivatives are summarized as below (Horikoshi et al. 1999):

1. Diffusion and (or) adsorption of the derivatives to the catalyst surface
2. Hydroxyl radical attack at ring atoms with greater electron densities
3. Conversion of C to CO_2, and N to NH^{4+}, NO^{3-}, and N_2, respectively.

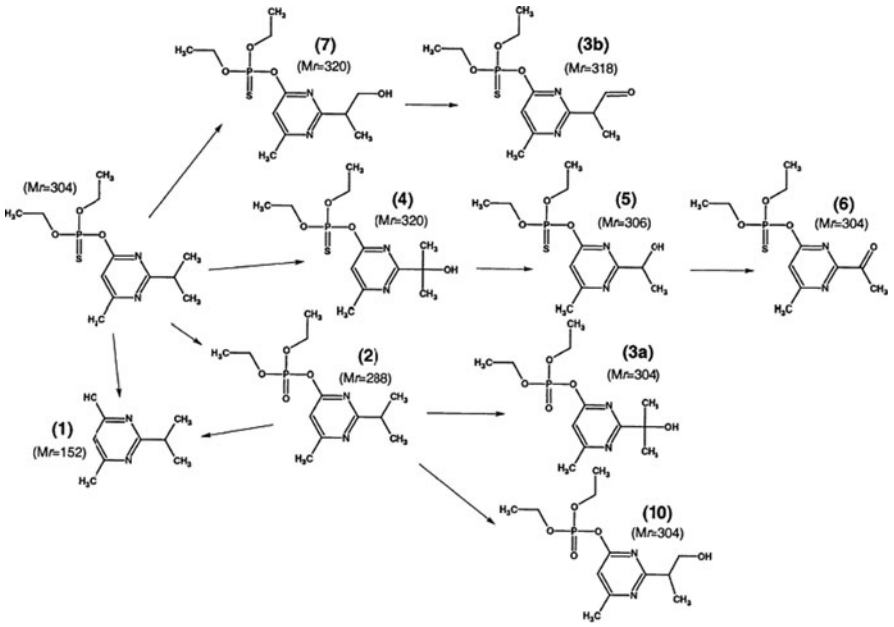

Fig. 6 Proposed degradation pathways for diazinon TiO_2 induced photocatalysis: IMP (1), diazoxon (2), hydroxydiazoxon (3a), diazinon aldehyde (3b), hydroxydiazinon (4), hydroxyethyl derivative of diazinon (5), diazinon methyl ketone (6), 2-hydroxydiazinon (7), and 2-hydroxydiazoxon (10). Reprinted from Kouloumbos et al. (2003), Copyright with permission from Elsevier

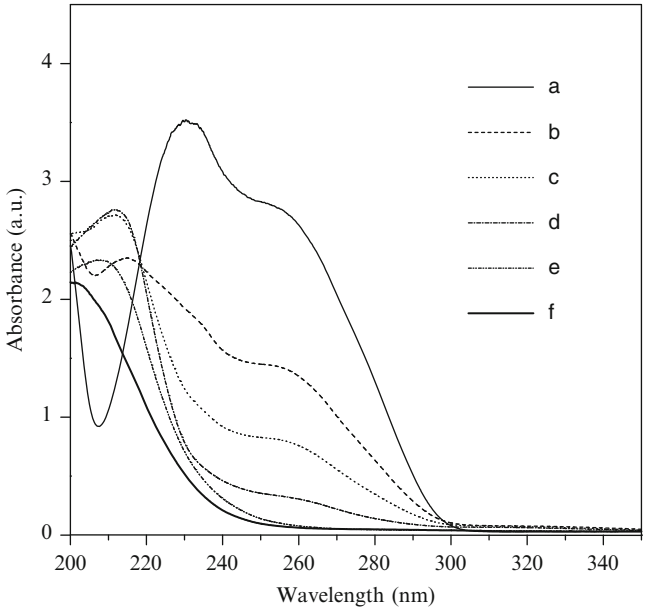

Fig. 7 Changes in the UV absorption spectrum of IMP after irradiation time of (a) 0 min, (b) 30 min, (c) 60 min, (d) 90 min, (e) 4 h, and (f) 8 h. Reprinted from Lee et al. (2003), Copyright with permission from Elsevier

3.2 pH Effect

The pH condition has been reported to affect the photocatalytic reaction rate. In the photocatalytic oxidation of pyrimidine base, the reaction rate is also influenced by the condition of pH. Pyrimidine bases such as thymine, 6-methyl uracil, and cytosine show lower reaction rates at higher pH values (Dhananjeyan et al. 1996, 1997, 2000b). The band edge positions of TiO_2 shift to more negative values with increasing pH, resulting in a decrease of oxidation potentials. Conduction and valence band edges increase at the rate of −60 mV per unit increase in pH under strongly basic conditions (Takeda et al. 1998). The dissociation of TiOH to TiO^- and H^+ in basic solution can cause low concentration of surface hydroxyl groups that produce active hydroxyl radicals. Also, the pyrimidine bases become negatively charged under basic conditions, and there is a decrease in the extent of adsorbability that leads to a decrease in the reaction rate. The pK_a value of the reaction represented as in (15) ($^{\bullet}O_2^- + H^+ \rightarrow {}^{\bullet}HO_2$) is reported to be about 4.88 (Wang et al. 1999). In the pH region above the pK_a value of HO_2 radicals (=4.88), the reverse reaction of (15) dominates and (16)–(20) do not proceed. As a result, the electron scavenging by oxygen decreases under strongly basic conditions.

IMP also shows reaction rate-dependency on the pH condition (Lee et al. 2003). Under strongly acidic conditions, non-bonding electrons can accept protons easily, and IMP exists as positively charged protonated species. On the other hand, dissociation of a proton from the IMP hydroxyl group happens readily under strongly basic conditions. The deprotonated IMP molecules exist as negatively charged species. Similar trend is also observed in other pyrimidine compounds. Some kinds of pyrimidinol compounds have two kinds of pK_a values. Acidic pK_a is about 6.78–9.17 and basic pK_a is about 1.87–2.24 (Brown and Mason 1962). The surface charge state of TiO_2 also depends on the pH condition. The isoelectric point of TiO_2 is located at about 6.5 of pH and the surface hydroxyl of TiO_2 exists as $TiOH_2^+$ and TiO^- forms, causing electrostatic repulsion between IMP and TiO_2 under strongly acidic and basic conditions, respectively. Therefore, the overall degradation rate constants under acidic, mildly acidic, and mildly basic conditions were higher than those under strongly acidic and basic conditions (see Table 1). In the case of pyridine derivatives, similar pH effect was observed (Nedoloujko and Kiwi 2000).

Table 1 Overall degradation rate constants of IMP by TiO_2 and SiO_x-loaded TiO_2 at different initial pH conditions (Lee et al. 2003)

	Initial pH					
	2		6.3		10	
Catalyst	k (min^{-1})	R^2	k (min^{-1})	R^2	k (min^{-1})	R^2
TiO_2 (P-25)	0.0127	0.9885	0.0223	0.9979	0.0073	0.9915
0.5 mol% SiO_x-loaded TiO_2[a]	0.0180	0.9898	0.0206	0.9906	0.0079	0.9901
0.5 mol% SiO_x-loaded TiO_2[b]	0.0196	0.9976	0.0185	0.9980	0.0079	0.9956

[a]Prepared by sol–gel method
[b]Prepared by impregnation method

The pH-dependent behavior of photocatalytic oxidation is explained as follows:

1. Nernstian shift of band edge position
2. Change in surface hydroxyl group concentration
3. Change in electron scavenging rate by O_2
4. Changes in surface charge state of TiO_2 and ionic state of reactant

3.3 *Effect of Metal Ion*

The existence of metal ions in solution affects the photocatalytic degradation rate of pyrimidine derivatives. For uracil and 6-methyluracil, an increase in the Ag^+ concentration enhances the photocatalytic degradation rate, reducing the extent of hole–electron recombination (Dhananjeyan et al. 1997). However, Cu^{2+} retards the photocatalytic decomposition rate. The retardation is attributed to the short-circuiting reaction (26) and (27) and metal deposition, causing hole–electron recombination and impediment of light absorption, respectively (Dhananjeyan et al. 2000a).

$$Cu^{2+} + e^- \rightarrow Cu^+ + e^- \rightarrow Cu \tag{26}$$

$$Cu + h^+ \rightarrow Cu^+ + h^+ \rightarrow Cu^{2+} \tag{27}$$

Fe^{3+} can also be used as an electron scavenger instead of oxygen. In photocatalytic degradation of IMP, rutile TiO_2 shows poor activity. In the presence of Fe^{3+}, however, photocatalytic decomposition of IMP over rutile TiO_2 occurs faster than anatase TiO_2 as shown in Table 2 (Lee et al. 2004). This result implies that conduction band position is responsible for the difference in activity between anatase and rutile. The standard redox potential of the $O_2/{\bullet}O_2^-$ is -0.33 V versus NHE and that of the Fe^{3+}/Fe^{2+} is +0.77 V versus NHE (Bamwenda et al. 2001). The conduction band of anatase ($E \approx -0.5$ V versus NHE) is more negative than both of the standard redox potentials above. However, the conduction band of rutile ($E \approx -0.3$ V versus NHE) (Lin et al. 1999) is more positive than the standard potential of $O_2/{\bullet}O_2^-$ and more negative than that of Fe^{3+}/Fe^{2+}. This suggests that photogenerated electron from rutile cannot react with oxygen thermodynamically, but can react with Fe^{3+}. As a result, rutile shows a poor activity in photocatalytic degradation of IMP when using oxygen as an electron scavenger, whereas it shows a good activity

Table 2 The activity comparison of photocatalytic degradation of IMP according to the kind of electron scavenger (Lee et al. 2004)

Electron scavenger	Oxygen	Ferric ion
CO_2 formation over anatase (μmol)	599	556
CO_2 formation over rutile (μmol)	56	614

with ferric ion. Lin et al. (1999) and Ohno et al. (2001) made similar conclusions in photocatalytic oxidations of acetone and 2-propanol, respectively.

Also, Fe^{3+} can be doped on TiO_2 to increase the photo-oxidation rate of pyrimidine bases. The maximum rate was observed with 0.75 at% of Fe^{3+} loading amount. Doped Fe^{3+} acts as an e^--trap and a transfer site to Ti^{4+}, preventing the recombination of h^+ and e^- (Dhananjeyan et al. 2000a).

3.4 *Effect of TiO_2 Property*

The photocatalytic activity of TiO_2 is generally influenced by physicochemical properties, including crystal structure, crystallinity, surface state, particle size, surface area, etc. (Porter et al. 1999).

Anatase TiO_2 generally shows higher activity than rutile TiO_2 in photocatalytic oxidations of organic compounds (Porter et al. 1999; Ding et al. 2000; Devi and Krishnaiah 1999; Jung and Park 1999; Hong et al. 2001). For IMP, a similar result was reported with oxygen as an electron scavenger (Lee et al. 2004).

The effect of crystallinity is related to the bulk defect. Higher crystallinity results in lower bulk defects, enhancing hole–electron separation by surface traps (Jung and Park 1999).

As mentioned in the earlier chapter, pH condition affects the photo-oxidation rate of pyrimidine derivatives due to the isoelectric point of TiO_2. The isoelectric point of TiO_2 can be controlled by surface modification. As shown in Fig. 8, The SiO_x loading on TiO_2 lowers the isoelectric point of TiO_2 (Lee et al. 2003; Lee 2004).

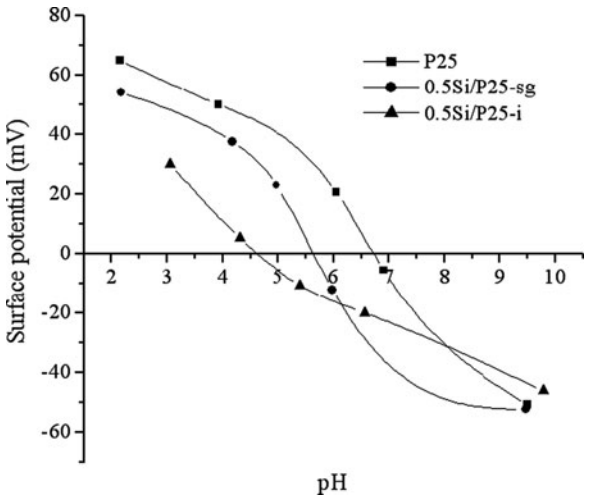

Fig. 8 Comparison of isoelectric point between pure TiO_2 and SiO_x-loaded TiO_2. Reprinted with permission from Ding et al. (2000), Copyright, American Chemical Society

Under strongly acidic conditions, SiO_x-loaded TiO_2 showed higher activity and less positive surface charge than pure TiO_2 (see Table 1). As a result, less electrostatic repulsion exists between the catalyst and the IMP molecule under strongly acidic conditions, resulting in a faster photocatalytic oxidation of IMP.

The channel-structured TiO_2 with pore size of about 18 nm is obtained by in situ esterification method using PEG as alcohol source without H_2O addition. The channel structure is originated from the organic–inorganic interaction between Ti species and PEG template, which enhances the photocatalytic activity for IMP decomposition (Oh et al. 2006).

Particle size is an important factor in determining the efficiency of the photocatalyst. This is related with surface area to affect adsorption ability and quantum size effect that change electronic structure. Especially when the particle size of semiconductor material such as TiO_2 is less than the De Broglie wavelength, quantum size effects take place depending on the specific electronic properties of the semiconductor, such as the effective masses of electrons and holes. Quantum size effects are as follows (1) blue shift of the fundamental absorption edge of the quantum size particle that can be controlled by tuning the particle size, and (2) enhanced photoredox potential for photogeneration of electrons and holes. These effects occur because of the physical confinements of electrons and holes in potential wells defined with the crystallite boundaries, typically ranging from 5 to 25 nm (Ollis and Al-Ekabi 1993). The quantum size effects of nano-sized TiO_2 have been widely studied (Anpo et al. 1987; Kormann et al. 1988; Choi et al. 1994; Serpone et al. 1995). When nano-sized TiO_2 particles are obtained using various mesoporous materials determining particle size, the bandgap increments due to quantum size effect are observed in both anatase TiO_2 and rutile TiO_2. The bandgap increment in rutile TiO_2 enhances the photocatalytic oxidation rate of IMP by virtue of the increase in redox potential of TiO_2. However, the bandgap increment in anatase TiO_2 does not affect the efficiency of IMP photocatalytic oxidation (Lee et al. 2005).

3.5 Application Field

Because pyrimidine derivatives are mainly found in DNA bases or pesticides, their photocatalytic oxidations are useful for the treatment of microorganisms, wastewater, ground water, etc. Some examples are listed below:

1. Analysis of DNA sequence (Dhananjeyan et al. 1996)
2. Waste/Ground water treatment from pesticide synthetic process (Kouloumbos et al. 2003; Lee et al. 2003)
3. Sterilization of microorganisms such as bacteria, fungi, mold, and virus (Fujishima et al. 2000)
4. Cancer treatment (Fujishima et al. 2000)

4 Phenol Compounds

It is well known that phenol compounds constitute an important family of priority pollutants in wastewater. Their presence has been confirmed in many different industrial wastewaters from chemical, petrochemical or even from food-processing industries. Due to their toxicity and hazardous property, phenols need to be removed from wastewater before its release into the aquatic environment. Biological oxidation is usually the cheapest and the best way to deal with concentrated wastewaters. However, phenols might present some inhibitory problems and early removal of these compounds is highly recommended. Chemical oxidation is one possible way to accomplish this task. Ozone processes or advanced oxidation processes have been proved to be appropriate technologies.

Beltrán et al. (2005) showed that photocatalytic ozonation ($O_3 + UV + TiO_2$) is more efficient method in removing phenols (phenol, 4-chlorophenol, and 4-nitrophenol) than ozonation (O_3), catalytic ozonation ($O_3 + TiO_2$), ozone photolysis ($O_3 + UV$), photocatalysis ($TiO_2 + UV$), and photolysis (UV). Table 3 lists the intermediates identified in different oxidation processes. As can be seen, with some exceptions, the nature of intermediates is similar regardless of the process applied. With the exception of benzoquinone, the organic intermediates can be grouped into three different categories: polyphenols such as resorcinol, catechol, and hydroquinone, unsaturated carboxylic acids such as fumaric and maleic acids, and saturated carboxylic acids such as glyoxylic, oxalic, and formic acids. Also, nitrogen as nitrate from 4-nitrophenol and chloride from 4-chlorophenol were detected in solution.

From kinetic data available in the literature (see Table 4) the following considerations can be postulated. On the one hand, given the initial concentration of phenols, it is believed that these compounds and some polyphenols are mainly removed during the first minutes of reaction through direct ozone attack: electrophilic substitution and 1,3-cycloaddition reactions. On the other hand, unsaturated and saturated carboxylic acids, especially the latter ones that are more refractory to the ozone attack, are likely to be removed through hydroxyl radical oxidation.

Table 3 Intermediates identified in the photocatalytic ozonation of phenols (Beltrán et al. 2005)

In phenol oxidation	In *p*-nitrophenol oxidation	In *p*-chlorophenol oxidation
Hydroquinone	Hydroquinone	Hydroquinone
Resorcinol	Resorcinol	Resorcinol
Benzoquinone	Benzoquinone	Benzoquinone
Catechol	–	–
–	Phenol	–
Oxalic acid	Oxalic acid	Oxalic acid
Maleic acid	Maleic acid	Maleic acid
Fumaric acid	Fumaric acid	Fumaric acid
Glyoxylic acid	Glyoxylic acid	Glyoxylic acid
–	Formic acid	Formic acid

Table 4 Rate constants of the direct reactions of ozone and hydroxyl radicals with phenols, and intermediates detected (Beltrán et al. 2005)

Organic compound	pH	k_D ($M^{-1}\,s^{-1}$)[a]	Ha	k_{HO} ($M^{-1}\,s^{-1}$)[b]
Phenol	6.1[c]	3.9×10^5	5.2	6.6×10^9
p-Chlorophenol	5[c]	4.2×10^4	1.4	7.6×10^9
p-Nitrophenol	4.7[c]	5.0×10^4	1.5	3.8×10^9
Hydroquinone	3.9[d]	1.5×10^6	2.9	10^{10}
	3[e]		3.7	
	3.1[f]		0.8	
Resorcinol	5[d]	9.8×10^4	0.1	1.2×10^{10}
	3[f]		0.3	
Catechol	3.9[d]	3.1×10^5	1.5	1.1×10^{10}
Fumaric acid	3.5[d]	6,000	0.05	1.1×10^9
	2.9[e]		0.1	
Maleic acid	3.9[d]	1,000	0.01	6×10^9
	2.9[e]		0.03	
	3[f]		0.03	
Glyoxylic acid	3.5[d]	1.34	0.005	NA
	3[e,f]	0.82	0.01	
Formic acid	3[e]	19.3	0.015	1.3×10^8
Oxalic acid	3.4[d]	0.04	0.0005	5×10^7
	2.9[e,f]		0.003	

[a]Rate constants of the direct reactions of ozone
[b]Rate constants of the direct reactions of hydroxyl radicals
[c]For the start of reaction
[d]In phenol oxidation
[e]In *p*-chlorophenol oxidation
[f]In *p*-nitrophenol oxidation

Table 5 Apparent pseudo-first-order rate constants of the oxidation of phenols referred to COD (Beltrán et al. 2005)

Oxidation system	Phenol ($k \times 10^2$ min^{-1})	*p*-Chlorophenol ($k \times 10^2$ min^{-1})	*p*-Nitrophenol ($k \times 10^2$ min^{-1})
O_3	0.47	0.57	0.43
O_3/UV	2.97	3.58	1.89
UV/TiO_2	0.11	0.55	0.24
O_3/TiO_2	0.54	0.59	0.35
O_3/UV/TiO_2	5.56	5.25	3.21

Apparent pseudo-first-order rate constants of the oxidation of phenols are tabulated in Table 5. Regardless of the phenols treated, rate constant values referred to COD for the O_3/UV/TiO_2 system are the highest among the oxidation systems studied. In general, the oxidation order of reactivity was 4-nitrophenol < phenol < 4-chlorophenol. It should be highlighted that the order of reactivity of the phenols

studied with ozone is highly dependent on the presence of activating–deactivating groups in the aromatic ring for electrophilic aromatic substitution reactions. Thus, theoretical order of increasing reactivity is 4-nitrophenol < 4-chlorophenol < phenol since the nitro and chlorine groups strongly and slightly, respectively, deactivate the ozone electrophilic reactions. Thus, from the results obtained, regarding ozone electrophilic reactions, negative effect of the nitro group seems clear while that of the chlorine is not so clear since a better reactivity is observed compared to phenol. On the basis of these results, the addition of TiO_2 to improve the removal of phenols is appropriate in cases where the phenol contributes some strong deactivating groups to the electrophilic substitution reactions.

4.1 Chlorophenols

Chlorophenols occur in all components of the natural environment. They result from a variety of sources: the natural chlorination of organic material, biodegradation of phyto-defensive chemicals, or the large-scale disinfection of drinking water. Chlorophenols are weakly acidic, therefore in the aquatic environment they occur in both dissociated and undissociated forms. The main photochemical processes involving chlorophenols are photodissociation, photoisomerization, photosubstitution, photorearrangement, photo-oxidation, and photoreduction. In general, the photodegradation of any substance in the natural environment is a superposition of reactions of several or all of these types, and its rate and quantum yield depend on a variety of factors. The maximum absorption level of the compound, wavelength of radiation, duration of radiation exposure, and physical state of the compound undergoing the transformation process play central roles in determining the photochemical processes. Because of the ubiquitous presence of chlorophenols in the natural environment and their toxic properties, understanding the kinetics and mechanisms of the process of photodegradation of these compounds is critically important. Czaplicka summarized direct photolysis and photodegradation of chlorophenols in the presence of hydroxyl radicals and singlet oxygen (Czaplicka 2006).

The rate of direct photolysis of chlorophenols is proportional to the irradiation intensity. Chlorophenols strongly absorb radiation at wavelengths between 230 and 300 nm. Various studies show that the rate of photolysis of chlorophenols depends on the pH of the reaction environment and on the structure of the molecule – particularly the position of the chlorine atom relative to the hydroxyl group. It is generally accepted that an observed reaction rate is a sum of the reaction rates of the undissociated and dissociated forms of the compound. It is also known that the reactivity of these forms differs considerably. Observational analysis has regularly found that dissociated forms are more reactive than undissociated ones (Benitez et al. 2000). An increase in the reaction rate constant with increasing pH was observed (Benitez et al. 2000; Shen et al. 1995). Photolysis rate constants for chlorophenols determined under some conditions are presented in Table 6 (Czaplicka 2006). Boule et al. (1982) found that during direct photolysis, the dechlorination rates of 4-chlorophenol (also

Table 6 Rate constants for direct photolysis of chlorophenols (Czaplicka 2006)

Compound	Rate constant (min^{-1})	pH
2-Chlorophenol	7.1×10^{-3}	3
	7.7×10^{-3}	5
	20×10^{-3}	7
	101×10^{-3}	11
2,4-Dichlorophenol	3.6×10^{-3}	3
	4.5×10^{-3}	5
	28.6×10^{-3}	7
	126×10^{-3}	11
2,4,6-Trichlorophenol	2.3×10^{-3}	3
	6.3×10^{-3}	5
	29.4×10^{-3}	7
	36.3×10^{-3}	11
Pentachlorophenol	0.16	3
	0.19	5
	0.21	7
	0.26	9

Reprinted from Czaplicka (2006), Copyright with permission from Elsevier

known as *p*-chlorophenol) and 2-chlorophenol are faster than 3-chlorophenol. Kuo (1999) observed that the reaction rate for direct photolysis upon irradiation at $\lambda < 300$ nm decreases in the order: 2,4-dichlorophenol > 4-chlorophenol > 2-chlorophenol. Shen et al. (1995), on the basis of results obtained under similar conditions, found that rate constants during direct photolysis decrease in the order: 2,4-dichlorophenol > 2-chlorophenol > 2,4,6-trichlorophenol. These results indicated that *para* and *ortho*positions are more active in direct photolysis. The increased occurrence of *para* position in comparison to *ortho* position in this reaction is explained by the intermolecular hydrogen bonding between the *ortho*-positioned Cl atom and the hydrogen from the hydroxyl group. In the case of *ortho*-substituted chlorophenols, hydrogen bonds may be formed internally between Cl and OH as well as externally between molecules of chlorophenol and water.

Besides photocatalysis, hydroxyl radicals can be formed through various chemical reaction pathways such as (1) irradiation of H_2O_2; (2) photolysis of ozone, through the generation of singlet oxygen atoms which then react with water to generate •OH; (3) photolysis of Fe^{3+} or polyoxometallates; (4) Fenton-type reaction of Fe^{+2}, Cu^{+1}, or Ti^{+3}; and (5) radiolysis of water. In the case of natural water, present protonic forms of nitrate and nitrous ions are sources of hydroxyl radicals. The organic matter dissolved in aquatic environment, especially humic acids, absorb a large portion of photons, which can also instigate the formation of hydroxyl radicals.

The reaction of chlorophenols and hydroxyl radicals is described by a second-order reaction model or as a pseudo-first-order reaction (Czaplicka 2006). Antonaraki et al. (2002), investigating the effect of the position of chlorine atom substitution on the reaction rate, found that the rate of photo-oxidation of

monochlorophenols (for $\lambda > 320$ nm) by the •OH radicals decreases according to the order: 3-chlorophenol > 4-chlorophenol > 2-chlorophenol. It was also observed that the presence of two chlorine atoms in *meta* positions of a molecule (3,5-dichlorophenol) – when compared to a chlorophenol with chlorine atoms in two *ortho* positions (2,6-dichlorophenol) – increases the rate of the reaction (Antonaraki et al. 2002; Moza et al. 1988). A similar phenomenon was reported for trichlorophenols. Trichlorophenols with two chlorine atoms in *meta* positions reacted faster than trichlorophenols with only one chlorine atom in the *meta* position. This means that for mono-, di-, and trichlorophenols, the initial rate of the reaction is affected more by positions of the substituted chlorine atoms than by the number of these atoms in a molecule. In the case of observed reactions of •OH radicals with pentachlorophenol, Mills and Hoffmann (1993) confirmed that the additions of •OH radicals to *ortho* positions were more favorable than additions to *para* positions. It may be concluded that the increase in the number of substituted chlorine atoms on the ring blocks the favorable positions susceptible to hydroxyl attack, which results in a decrease in the degradation rate with increased number of chlorine atoms in the molecule.

Singlet oxygen is the first excited state of molecular oxygen. As a moderately reactive electrophile, it oxidizes numerous electron-rich organic substances. The method most frequently used for producing singlet oxygen in the laboratory is photosensitization. Both continuous irradiation and pulsed excitation studies have made much use of this method for singlet oxygen generation. Singlet oxygen in natural waters can also be produced in aqueous solutions of an appropriate sensitizer that absorbs light and transfers the energy to the dissolved triplet oxygen. The dissolved organic matter is a primary sensitizer responsible for the singlet oxygen formation.

Tratnyek and Holgné (1991), investigating reactions of chlorophenols with singlet oxygen using rose bengal as a sensitizer, observed that *ortho* and *meta* positions in monochlorophenol molecules were more active in reactions with singlet oxygen, independent of the presence of dissociated or undissociated forms. They also showed that increasing the number of chlorine atoms caused a decrease in the rate of the reaction.

Ozoemena et al. (2001), studying photosensitization transformations of polychlorophenols by radiation above 600 nm, suggested that negative inductive effects (when halogen substitution occurs on an aromatic ring) result in an electron-withdrawing effect from the benzene nucleus, deactivating it for an electrophilic attack by singlet oxygen. This electron withdrawal decreases the contribution of the type II pathway as the number of halogen substitutes increases. However, in the case of polychlorophenols, the electron-withdrawing effects of chlorine substituents cause a reduction in the electron donating ability of the substrate while the electron acceptor's ability is increased substantially.

Sakthivel and Kisch (2003) indicated that nitrogen-doped TiO_2 showed much better activity for the photocatalytic oxidation of 4-chlorophenol with visible light ($\lambda \geq 455$ nm). Three N-doped TiO_2 were prepared by hydrolysis of titanium tetrachloride with a nitrogen-containing base, such as ammonia, ammonium carbonate, or ammonium bicarbonate, respectively, followed by calcination in air

at 400°C. The slightly yellow resultants contained 0.08–0.13 wt% of nitrogen. In addition, the doped materials exhibited bandgap energies of 3.12 ± 0.01 eV, which suggested that a slight reduction in the bandgap, about 0.02 eV, was achieved compared to the undoped TiO_2. The nitrogen-doped materials all photocatalyzed the mineralization of 4-chlorophenol with artificial visible light ($\lambda \geq 455$ nm). About 50% conversion was observed after 6 h, whereas less than 1% of mineralization occurred in the case of unmodified titanium dioxide. The initial degradation rates were about 10–20 times larger.

Visible light-assisted photomineralization of 4-chlorophenol was also performed by TiO_2 modified with platinum(IV) chloride (Burgeth and Kisch 2002). 4 wt% Pt/anatase TiO_2 was the best photocatalyst in comparison with anatase–rutile mixed TiO_2 (commercial name P-25), unmodified anatase TiO_2, and 1.1 wt% Pt/P-25, showing a six fold higher activity than that of P-25 ($\lambda \geq 455$ nm). Upon UV irradiation ($\lambda \geq 320$ nm), 4 wt% Pt/anatase TiO_2 was even more active than P-25. It was postulated that chemisorption of $[PtCl_6]^{2-}$ onto high surface area anatase TiO_2 powder led to the formation of a covalently bound surface complex. This novel hybrid semiconductor was an efficient photocatalyst for the mineralization of 4-chlorophenol both with visible and UV light. Activity was retained even in diffuse indoor light.

In general, the number and positions of chlorine atoms strongly influence the kinetics and mechanism of the chlorophenol photodegradation. Position of substituent chlorine atoms in the molecule is a key determinant in the reaction kinetics. In the case of direct photolysis, favorable positions are *para-* and *ortho-* due to the inductive and mesomeric effects of OH and Cl groups. When hydroxyl radicals are generated upon irradiation, the presence of a chlorine atom in *meta* position of monochlorophenols increases the reaction rate between chlorophenol and •OH. In the case of polychlorophenols, additions of hydroxyl radicals to *ortho* positions are more favorable than *para* positions. In addition, steric effects are very important for polychlorophenols.

4.2 Nitrophenols

Nitrophenols are common refractory pollutants that can be present in industrial wastewaters. In particular, effluent wastewater from the synthetic dye, petrochemical, pesticide, herbicide, and insecticide industries contain 4-nitrophenol (also known as *p*-nitrophenol) as a major pollutant (>10 ppm). The pollutant is also listed among the top 114 organic pollutants by the United States Environmental Protection Agency (USEPA). The feasibility of 4-nitrophenol-containing wastewaters being subjected to an ozonation process was investigated, whereas catalytic oxidation in a temperature range of 150–190°C was studied. Investigations on the photocatalytic abatement of 4-nitrophenol in TiO_2 aqueous slurries have also appeared in the literature (Lea and Adesina 2001; Andreozzi et al. 2000).

Lea and Adesina (2001) used an internally irradiated annular photoreactor to investigate the oxidative degradation of aqueous 4-nitrophenol with TiO_2 as the photocatalyst. The kinetics was determined as a function of nitrophenol concentration, oxygen partial pressure, catalyst loading, pH, temperature and light intensity. The photocatalytic oxidation of 4-nitrophenol was characterized by a relatively low activation energy of 7.83 kJ/mol, although transport intrusions were negligible. Rate decreased almost exponentially with pH while a quadratic behavior with respect to both oxygen pressure and nitrophenol concentration was symptomatic of self-inhibition. Possible explanation for this behavior is the formation of intermediates that competitively adsorb on similar sites to the reactants. Increased catalyst dosage also improved the reaction rate, although the possible effects of light scattering and solution opacity caused a drop at higher loadings. Rate, however, had a linear dependency on light intensity, suggesting that electron–hole recombination processes were negligible at the conditions studied. It was suggested that the photodegradation of 4-nitrophenol proceeded via aqueous dissociation to produce nitrophenoxide anions that subsequently adsorb on photogenerated holes and are attacked by hydroxide ions on the surface to yield oxygenated products as follows:

$$C_6H_5NO_3(aq) \leftrightarrow C_6H_4NO_3^-(aq) + H^+(aq) \tag{28}$$

$$TiO_2 + h\nu \rightarrow h^+ + e^- \tag{29}$$

$$H_2O + h^+ \rightarrow {}^\bullet OH(ads) + H^+(aq) \tag{30}$$

$$O_2 + e^- \rightarrow O_2^-(ads) \tag{31}$$

$$O_2^-(ads) + H^+(aq) \rightarrow HO_2^\bullet(ads) \tag{32}$$

$${}^\bullet OH(ads) \leftrightarrow OH^-(aq) + h^+ \tag{33}$$

$$C_6H_4NO_3^-(aq) + h^+ \leftrightarrow C_6H_4NO_3^\bullet(ads) \tag{34}$$

$$C_6H_4NO_3^\bullet(ads) + {}^\bullet OH(ads) \rightarrow NO_3^-(aq) + C_6H_5O^\bullet(ads) + h^+ \tag{35}$$

$$C_6H_5O^\bullet(ads) + HO_2^\bullet(ads) \rightarrow R_1COO^\bullet(ads) + R_2CO^\bullet(ads) \tag{36}$$

$$H^+(aq) + NO_3^-(aq) \leftrightarrow HNO_3(aq) \tag{37}$$

$$C_6H_5O^\bullet(ads) + HNO_3(aq) \rightarrow \text{N - containing oxygenated products} \tag{38}$$

$$R_1COO^\bullet(ads) + {}^\bullet OH(ads) \rightarrow H_2O + CO_2 + \text{low mol wt products} \tag{39}$$

$$R_2CO^\bullet(ads) + HO_2^\bullet(ads) \rightarrow H_2O + CO_2 + \text{low mol wt products} \tag{40}$$

$$h^+ + e^- \rightarrow TiO_2 + \text{heat} \tag{41}$$

where h^+ and e^- are photogenerated holes and electrons, respectively, while R_1 and R_2 are alkyl groups.

5 Pesticides

Pesticide pollution of environmental waters is a pervasive problem with widespread ecological consequences. The major sources of pollution by pesticides are wastewater from agricultural industries and pesticide plants. Wastewater from those sources may contain pesticides at levels as high as several hundred mg/L. Whatever the concentration level detected, pesticides have to be removed either to protect our water resources or to achieve drinking water quality. The main characteristics of this wastewater are its extreme toxicity, low volume and well-defined location. Suitable treatment is therefore required to decontaminate it, which is much easier than cleaning up subsequent environmental hazards. Possible treatment methods include physical entrainment (e.g., activated carbon filtration, membrane technologies), biodegradation, and chemical reactions. Entrainment is losing acceptance as a final solution for waste disposal because of its low efficiency when dealing with high concentration of pollutants. Moreover, entrained pollutants must be further treated for complete destruction. Some form of biological processing is usually the preferred method for the treatment of effluents containing organic substances, since biological treatment techniques are well established and relatively cheap. However, these biological methods are susceptible to toxic compounds that inactivate the waste-degrading microorganisms. In such cases, a potentially useful approach is to partially pretreat the toxic waste by oxidation technologies to produce intermediates that are more readily biodegradable. Many oxidation processes are currently employed for this purpose, including photocatalytic processes (TiO_2/UV), photochemical degradation processes (UV/O_3, UV/H_2O_2), and chemical oxidation processes (O_3, O_3/H_2O_2, H_2O_2/Fe^{2+}).

Pesticides, including herbicides, are classified and listed in terms of the characteristic structural groups in the review paper on photocatalytic transformation of pesticides in aqueous TiO_2 suspensions by Konstantinou and Albanis (2003). Among them, some chemical structures of pesticides are shown in Fig. 9 (Malato et al. 2000).

In order to assess the degree of mineralization reached during advanced oxidation processes (AOPs), the decrease of the total organic carbon (TOC) is generally estimated. Monitoring for chloride, nitrate, phosphate or ammonium ions using ion chromatography methods also provides useful data to follow the pesticide degradation. On the basis of the efficiency of AOPs, Chiron et al. (2000) concluded as follows:

1. Whatever the degradation system used, parameters linked to experimental conditions and reactor design are decisive in assessing the pesticide degradation rates. Among these parameters, light sources or ozone generator characteristics, treated water volumes, initial pesticide concentrations, details of analytical procedures, and types of equipments are especially relevant.

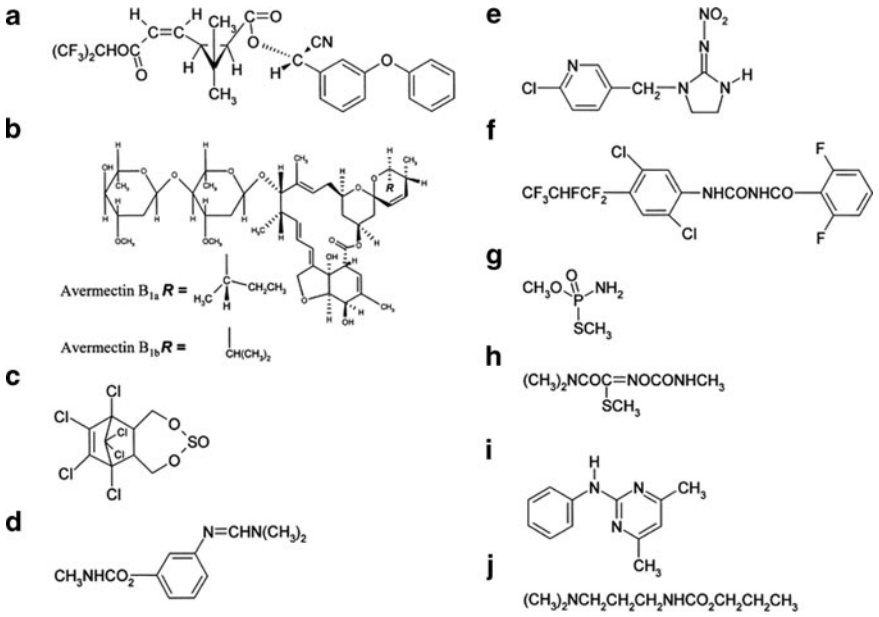

Fig. 9 Structures of the active ingredients in selected pesticides: (**a**) acrinathrin, (**b**) avermectine B1, (**c**) endosulfan, (**d**) formetanate, (**e**) imidacloprid, (**f**) lufenuron, (**g**) methamidophos, (**h**) oxamyl, (**i**) pyrimethanil, and (**j**) propamocarb (Malato et al. 2000). Reprinted from Malato et al. (2000), Copyright with permission from Elsevier

2. Higher degradation times can be logically expected when formulated compounds are used instead of pure active ingredients because the chemical composition of water can influence the efficiency of the process. For example, carbonate ions and dissolved organic matter are well-known scavengers of hydroxyl radicals, hence reducing the degradation rates.
3. Efficiency is usually not the bottleneck in the application of chemical oxidation processes for the elimination of contaminants from wastewaters. Nevertheless, the mineralization rate is usually much slower than the rate of pesticide disappearance, and total mineralization is not always achieved, indicating the importance of intermediate decomposition products. Toxic intermediates can be generated and incorporated into the effluent. Formation and decomposition kinetics of the intermediates, and identification of these by-products need to be established in order to (a) determine which specific compounds will appear in the effluent, (b) increase our understanding of the degradation pathways, and (c) establish which step is limiting the overall reaction rate.
4. Different oxidants generally lead to different intermediates and different final products. It is important to distinguish reactions that occur by a common pathway (e.g., the hydroxyl radical mechanism) or from other steps such as ozone oxidation, direct hole attack, or even direct photolysis.

Selected representative compounds of the pesticide family are introduced below.

5.1 s-*Triazines*

s-Triazine herbicides such as atrazine, simazine, trietazine, prometon, and prometryn were rapidly degraded within several minutes but full mineralization was not observed during the photocatalytic oxidation process. Figure 10 shows the proposed degradation pathways of atrazine, (2-chloro-4-(ethylamino)-6-(isopropylamino)-*s*-triazine), which is widely used for weed control in the cultivation of corn and other crops (Ziegmann et al. 2006). Pathways for *s*-triazine transformation include displacement of the substituent at position 2, side alkyl chain oxidation, and further dealkylation and deamination. Different intermediates have been identified, mainly hydroxylated and dealkylated derivatives, ammeline, and cyanuric acid being the common final photoproducts of all herbicides. The first reaction that takes place is the oxidation of the lateral chains, which yields acetamido and dealkylated derivatives as the main degradation products. Subsequent reactions are substituent hydrolysis reactions at position two and the final displacement of amino groups with hydroxyl groups, yielding cyanuric acid. The dealkylation mechanism follows the photo-Kolbe decarboxylation pattern through the formation of corresponding alcohol, aldehyde, and acid derivatives. Although the disappearance of initial compounds is very fast, the formation of the final product may require a relatively long irradiation time. In particular, substitution of the triazine ring-linked amino groups with hydroxy groups is a very slow process (Konstantinou and Albanis 2003). Moreover, reductive degradation paths that lead to dehalogenated *s*-triazines have been reported (Ollis and Al-Ekabi 1993; Minero et al. 1996).

Lackhoff et al. reported the induced degradation of atrazine on TiO_2- and ZnO-modified cement samples. The photocatalytic activity of the particles was determined by measuring the degradation rates of atrazine in comparison to unmodified cement samples (Lackhoff et al. 2003). Three kinds of TiO_2 were used to prepare 10 wt% TiO_2-modified cement samples: Degussa P-25, Hombikat UV 100, and anatase Jenapharm. For the atrazine degradation by irradiation of pure semiconductors and semiconductor-modified cement samples, the first-order rate coefficients were as shown in Fig. 11. Atrazine degradation rate was significantly enhanced due to the addition of 10 wt% Degussa P-25 and Hombikat UV 100 to Portland cement. The rate of Atrazine degradation by cement samples modified with 10 wt% anatase Jenapharm was increased only slightly in comparison to unmodified cement samples. The order of photocatalytic efficiency observed for different pure TiO_2 samples (Degussa P-25 > Hombikat UV 100 > anatase Jenapharm) compares well with the results obtained from modified cement samples. Drastic increase in pH caused by the presence of cement is speculated to be the potential reason for comparatively high reductions in photocatalytic efficiencies of modified cement samples. The pH values of pure metal oxide suspensions were in the range of pH 4.5–8.0 (4.9 for Degussa P-25, 5.5 for Hombikat UV 100, 4.5 for anatase Jenapharm, and 8.0 for ZnO), whereas all (modified) cement samples exhibited pH values of 12.5. At pH values greater than the pHpzc (point of zero charge, pH 6.3–6.6) TiO^- dominated the surface, whereas slightly alkaline atrazine ($pK_a = 1.6$) was less

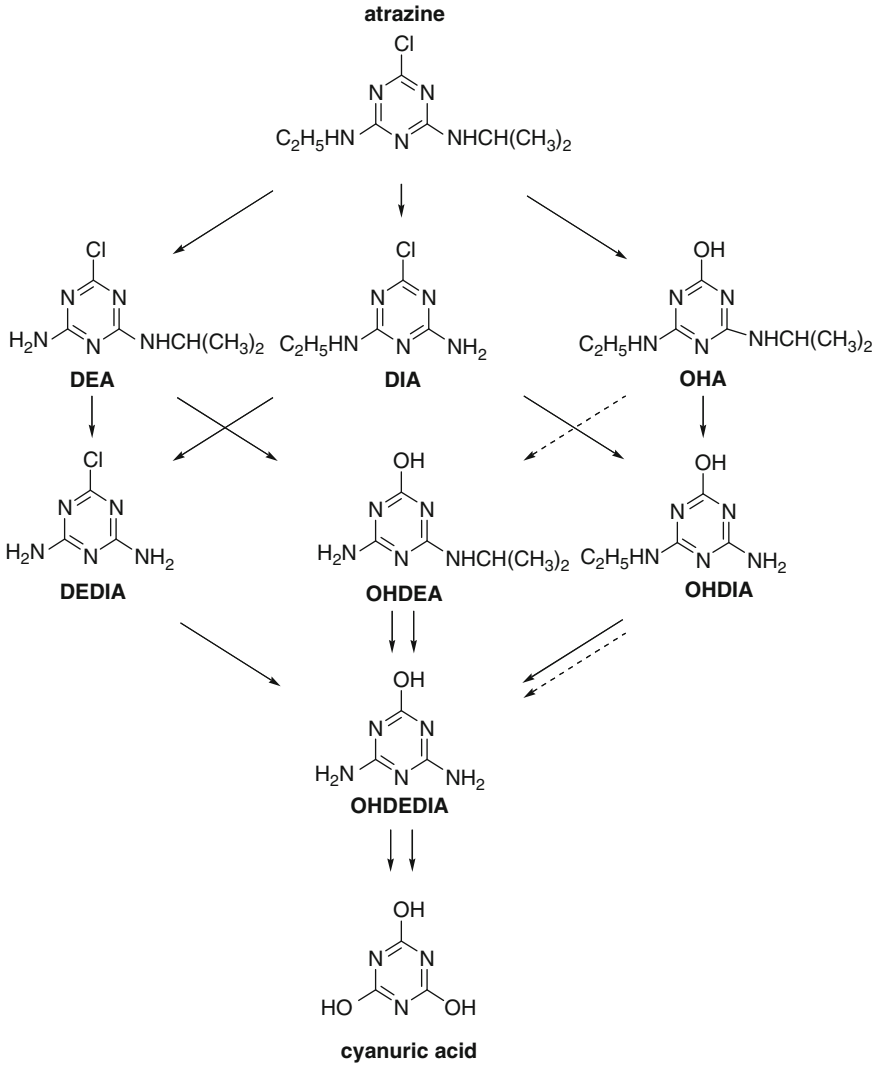

Fig. 10 Degradation pathways of atrazine (Ziegmann et al. 2006)

adsorbed due to electrostatic repulsion. The influence of the pH value is confirmed by the fact that photocatalytic activity of metal oxides with higher pH (Hombikat UV 100) is less retarded due to cement mixing (remaining activity of 7.8%) than metal oxides with lower pH (Degussa P-25 and anatase Jenapharm).

Upon photocatalytic treatment, sulfonylureas show similar behavior as *s*-triazines since they possess the characteristic *s*-triazine moiety in their molecules together with an aryl group and a sulfonylurea bridge. Three categories of photoproducts can be distinguished (see Fig. 12): The first one arises from the aromatic ring attack by •OH, leading to the hydroxylation of the benzene ring. Hydroxylated aromatics are more

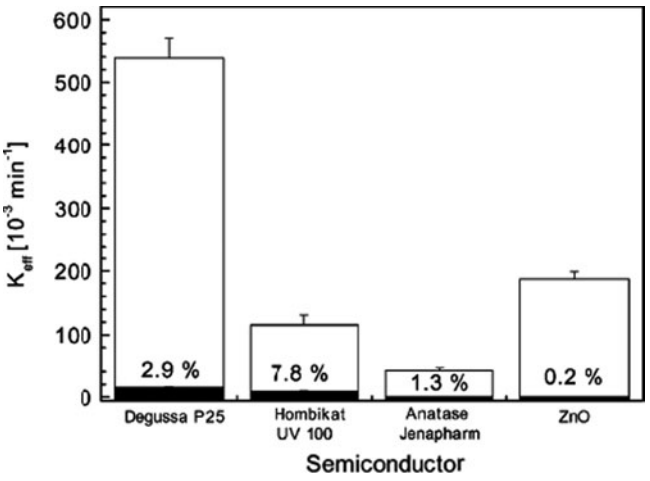

Fig. 11 First-order rate coefficients of atrazine degradation by irradiation of pure semiconductors (*white column*) and cement samples modified with these semiconductors (*black column*). The percentage values represent remaining photocatalytic efficiencies of modified cement samples in comparison to the belonging pure metal oxides. Reprinted from Lackhoff et al. (2003), Copyright with permission from Elsevier

easily oxidized than their parent compounds, and the reaction proceeds rapidly with further hydroxylation and ring opening. The second product family results from different cleavages of the sulfonylurea functional group to give various compounds containing a triazine ring. Finally, the third product class emerges from the photocatalytic degradation of *s*-triazine byproducts, as in the case of *s*-triazine herbicides, with ammelide and cyanuric acid being the final products. The degradation of both aliphatic and aromatic groups in sulfonylurea degradation lead to the formation of smaller and more oxidized metabolite molecules, such as short carboxylic acids (formic, acetic and oxalic) identified by LC–MS (Vulliet et al. 2002).

5.2 Phenylureas

Phenylurea and its derivatives have been used in weed control since the early 1950s because it was believed to inhibit photosynthesis of plants upon absorption by the roots. Their general structure and selected examples are shown in Fig. 13 (Amorisco et al. 2006; López et al. 2005). Phenylureas are highly persistent systemic herbicides, with half-lives of several months in soil, and are metabolized in vivo by soil microbes, plants, and animals via demethylation and hydroxylation. In recent years, the relatively high photochemical stability and water solubility of phenylurea herbicides have raised urgent questions about their role as persistent pollutants in soil and water, with consequent risks in the preservation of water supplies. Human health risks arising from water contamination by phenylurea herbicides is increased

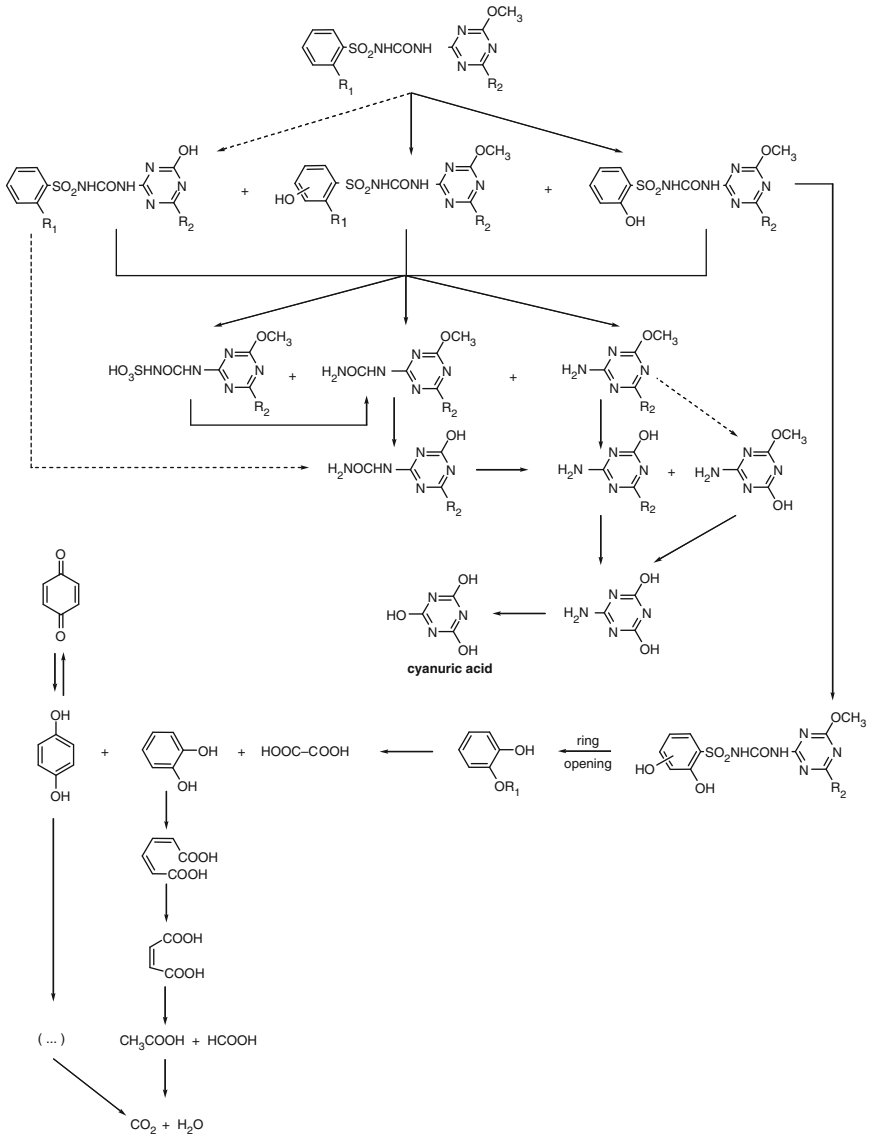

Fig. 12 Proposed pathway of photocatalytic degradation of sulfonylurea herbicides. Reprinted from Vulliet et al. (2002), Copyright with permission from Elsevier

upon considering the intensified toxicity of their by-products that are generated during water disinfection processes based on oxidants such as chlorine (hypochlorite) or ozone.

The photocatalytic transformation of phenylurea herbicides leads to the formation of several products. That results from (a) attack of the hydroxyl radicals on the aromatic ring and (b) abstraction of hydrogen atoms of the methyl group followed

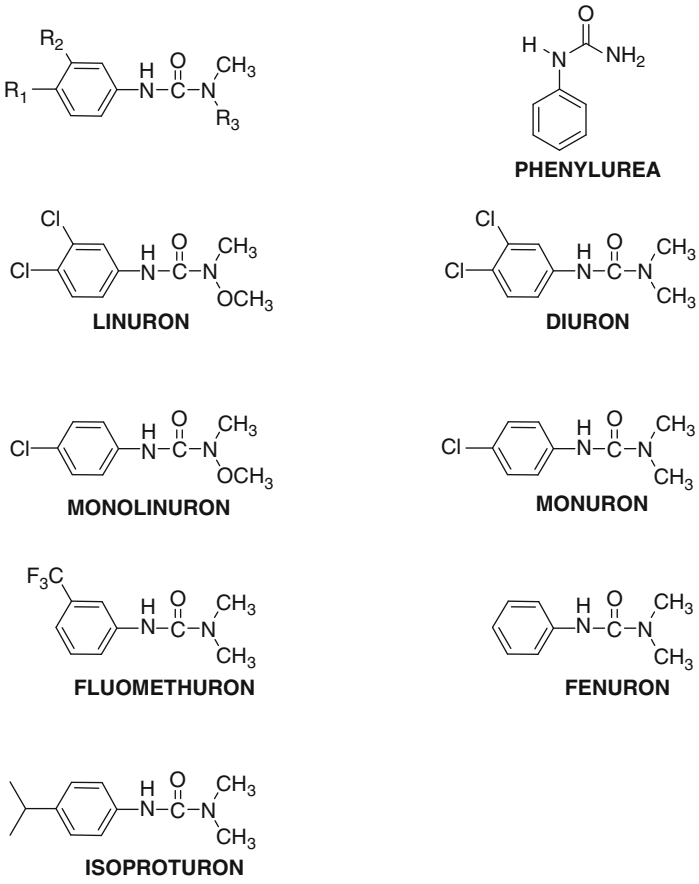

Fig. 13 General structure of phenylureas and selected examples (Amorisco et al. 2006; López et al. 2005)

by the addition of oxygen and decarboxylation, leading to the formation of dealkylated products. The distribution of products greatly depends on the pH of the medium. In neutral medium, the attack of the hydroxyl radicals is located both on the aromatic ring and on the methyl groups. In acidic medium, it is mainly located on the methyl groups, hydroxylation of the aromatic ring being clearly disfavored upon a decrease in pH.

López et al. (2005) compared the mechanism of TiO_2 photocatalytic degradation of Diuron (3-(3,4-dichlorophenyl)-1,1-dimethylurea) in aqueous solution compared with that of direct UV photodegradation. The radical anions, phenylurea$^{\bullet -}$, generated by one-electron reduction have $pK_a \approx 5$. From the rate constants of one-electron reduction, it can be deduced that the generation of phenylurea$^{\bullet -}$ and $O_2^{\bullet -}$ on the surface of photocatalysts may be competitive. HO• reacts with phenylureas via addition to the aromatic ring and/or hydrogen abstraction from a saturated carbon atom (98%), rather than one-electron oxidation (2%). Adsorption studies on TiO_2

show that photocatalysis is independent of the specific area of the catalyst. A variety of compounds have been observed upon photocatalytic degradation of Diuron, while only two hydroxychloro derivatives (refer to Fig. 14b) were generated after direct 365 nm irradiation (main emission wavelength of a medium-pressure mercury lamp). The photocatalytic degradation proceeds by three main pathways (1) oxidation of the side chain methyl group, (2) hydroxylation of the aromatic ring, and (3) dechlorination (see Fig. 14). Different photoproducts of photocatalytic degradation are found depending on the polymorphic form of TiO_2 used, the reason for this being unclear.

Amorisco et al. studied the photocatalytic degradation of chlortoluron (3-(3-chloro-4-methylphenyl)-1,1-dimethylurea) and chloroxuron (3-[4-(4-chlorophenoxy)phenyl]-1,1-dimethylurea) under solar irradiation, using TiO_2 embedded into polyvinylidene fluoride transparent matrix as a heterogeneous photocatalyst (Amorisco et al. 2006). The structures of several by-products were obtained using ion trap tandem mass spectrometry coupled to high-performance liquid chromatography through an electrospray ionization interface. The most important and typical by-products were hydroxylated compounds arising from the interaction between hydrogen atoms either on aromatic or aliphatic carbons of the two chlorinated herbicides and OH radicals generated on the TiO_2 surface under irradiation. Other by-products were generated by slightly different processes, namely demethylation, dearylation, and dechlorination, eventually followed by the interaction with OH radicals. They could be more effective precursors than the herbicides themselves towards an extensive degradation of these two chlorinated.

Amorisco et al. also hypothesized a possible scheme of photocatalytic degradation of isoproturon (3-(4-isopropylphenyl)-1,1-dimethylurea) (Amorisco et al. 2005). Like other phenylureas exemplified above, most byproducts resulted from single or multiple hydroxylation (by photogenerated OH radicals) of the isoproturon molecule at different positions. Meanwhile, substitution of some functional groups of the herbicide (isopropyl or methyl) by OH radicals was also observed.

It has been reported that the extent of adsorption on TiO_2 is not decisive in the degradation process, and photocatalytic reactions may take place independently of the degree of adsorption of phenylureas. Correlation analysis showed that the reactivity of different phenylureas upon TiO_2 heterogeneous photocatalysis is associated with polar effects of the substituents in the aromatic ring. However, the aqueous photocatalytic degradation of Monuron (3-(4-chlorophenyl)-1,1-dimethylurea) has been found to follow Langmuir–Hinshelwood kinetics, thus leading to complete mineralization of the pollutant for $3 < pH < 9$, but only partial mineralization at acidic and alkaline pH, even with longer irradiation times.

Unlike phenylureas, alkylureas undergo different transformation schemes. Urea and alkylureas are building blocks of several anthropogenic compounds, such as pesticides and fertilizers, natural compounds like caffeine, constituents of drugs, antiepileptic and HIV drugs, and transformation products of DNA. In addition, they have been identified as final products of natural degradation. Calza et al. (2006) summarized the photocatalytic transformation pathways followed by methyl- and ethylurea derivatives (see Fig. 15). Both the methyl- and ethylurea derivatives have been shown to easily degrade in the presence of titanium dioxide with similar

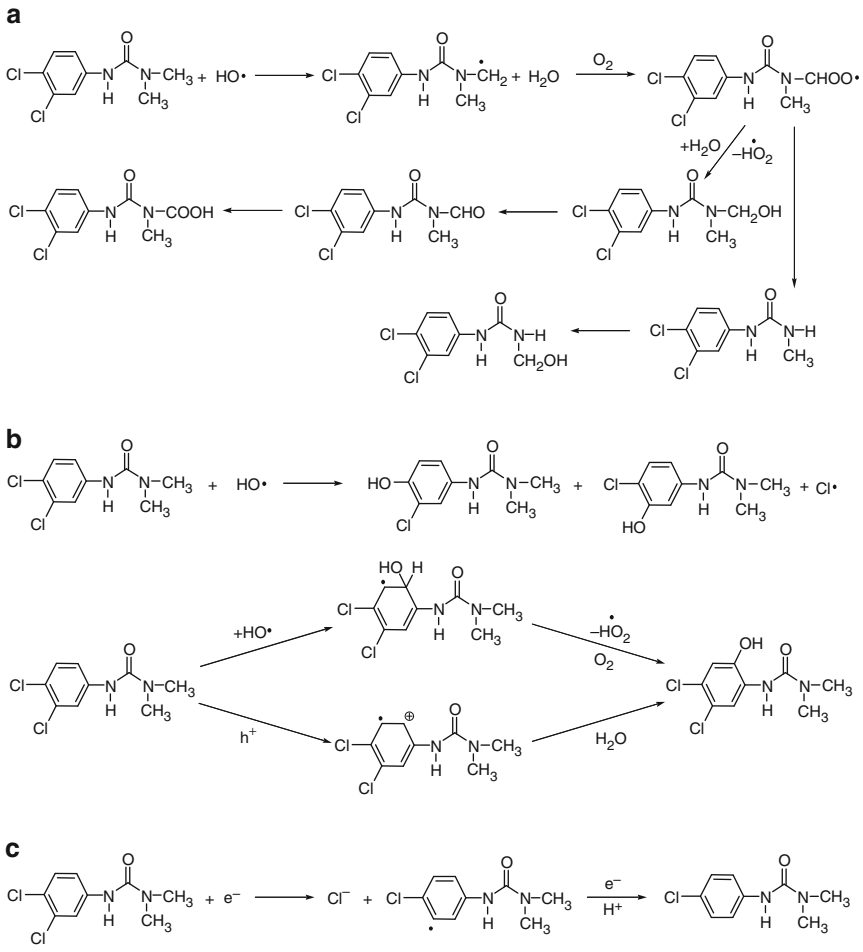

Fig. 14 Proposed pathway of photocatalytic degradation of phenylurea Diuron: (**a**) oxidation of the alkyl side chain, (**b**) chlorine substitution and hydroxylation of the aromatic ring, and (**c**) dechlorination (López et al. 2005)

kinetics, independent of the entity and the nature of the substitution. In contrast, the types of the formed intermediates and the rate and extension of the final mineralization are strongly dependent on the number of methyl or ethyl groups. These observations have been rationalized within the framework of a transformation mechanism in which all the investigated molecules (and the recognized intermediate compounds) are involved. In all cases, N-demethylation represents only a secondary pathway, while the main transformation proceeds by means of the unexpected cyclization of methylurea (MU), 1,1′-dimethylurea, 1,3′-dimethylurea (1,1′- and 1,3-DMU), ethylurea (EU), and 1,3′-diethylurea (1,3′-DEU) with the formation of (methyl)-amino-2,3-dihydro-1,2,4-oxadiazol-3-one as the major intermediate. Furthermore, the presence of an electron-donor group, such as a methyl or

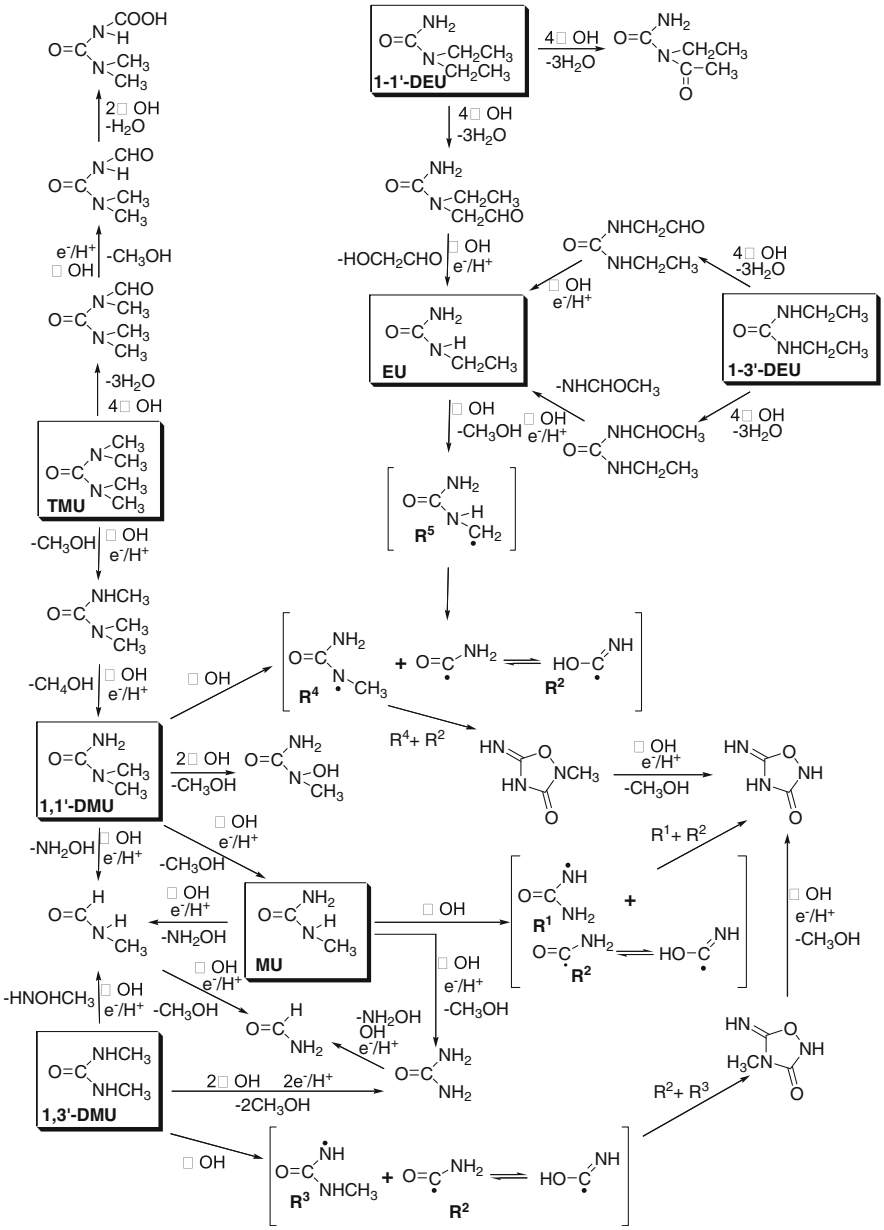

Fig. 15 Photocatalytic transformation pathways followed by methyl- and ethylurea derivatives (*1,1′-DEU* 1,1′-diethylurea, *TMU* tetramethylurea, *EU* ethylurea, *1,3′-DEU* 1,3′-diethylurea, *1,1′-DMU* 1,1′-dimethylurea, *MU* methylurea, *1,3′-DMU* 1,3′-dimethylurea) (Calza et al. 2006)

an ethyl group, favors both the release of the nitrogen atom (oxidation state −3) in the form of nitrate (oxidation state +4) and the mineralization of carbon, with respect to the unsubstituted urea.

6 Other Nitrogen-Containing Organic Compounds

6.1 Synthetic Dyes

Synthetic dyes are extensively used in many fields of up-to-date technology, e.g., in various branches of the textile industry, of the leather tanning industry in paper production, in food technology, in agricultural research, in light-harvesting arrays, in photoelectrochemical cells, and in hair colorings. Moreover, synthetic dyes have been employed for the control of the efficacy of sewage and wastewater treatment, for the determination of specific surface area of activated sludge for ground water tracing, etc. Synthetic dyes exhibit considerable structural diversity. Figure 16 shows synthetic dyes frequently studied in degradation researches (Forgacs et al. 2004).

Unfortunately, the exact amount of dyes produced in the world is unknown. It is estimated to be over 10,000 tons per year. Exact data on the quantity of dyes discharged in the environment are also unavailable. It is assumed that a loss of 1–2% in production and 1–10% loss in use are a fair estimate. For reactive dyes, this figure can be about 4%. Due to large-scale production and extensive application, synthetic dyes can cause considerable environmental pollution and are serious health-risk factors. Therefore, the growing impact of environmental protection on industrial development promotes the development of eco-friendly technologies, reduced consumption of freshwater, and lower output of wastewater. The release of significant amounts of synthetic dyes to the environment causes public concern and legislative problems, being a serious challenge to environmental scientists.

Decolorization of dye effluents has therefore received increasing attention. For the removal of dye pollutants, traditional physical techniques (adsorption on activated carbon, ultrafiltration, reverse osmosis, coagulation by chemical agents, ion exchange on synthetic adsorbent resins, etc.) can generally be used efficiently.

Nevertheless, these non-destructive techniques only transfer organic compounds from water to another phase, thus causing secondary pollution. Consequently, expensive operations such as regeneration of the adsorbent materials and post-treatment of solid-wastes are needed. Due to the large amount of aromatics present in dye molecules and the stability of modern dyes, conventional biological treatment methods are ineffective in decolorization and degradation. Furthermore, the majority of dyes are only adsorbed on the sludge and are not degraded. Chlorination and ozonation are also being used for the removal of certain dyes but at slower rates, as they often have high operating costs and limited effect on carbon content. Therefore, advanced oxidation processes that are able to degrade dye molecules in aqueous systems have been developed extensively during the last decade. Among these processes, heterogeneous photocatalysis using TiO_2 as photocatalyst appears

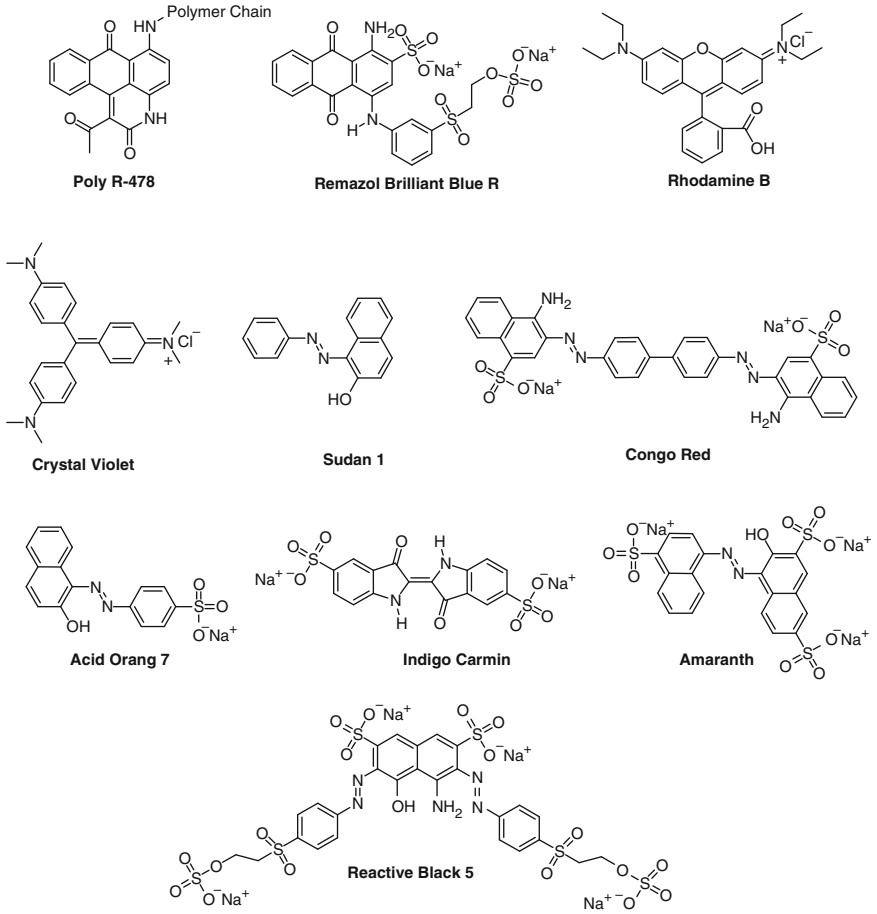

Fig. 16 Chemical structures of synthetic dyes frequently studied in degradation experiments. Reprinted from Forgacs et al. (2004), Copyright with permission from Elsevier

to be the most promising destructive technology. Various dyes, erythrosin B, eosin, Rose Bengal, rhodamine B, cresyl violet, thionine, chlorophyllin, anthracene-9-carboxylic acid, porphyrins, phthalocyanines, and carbocyanines have been reportedly employed as sensitizers. In these examples, the redox couples are often employed to regenerate the sensitizer (Cho et al. 2001). If one restricts such a regeneration process, the sensitizer undergoes oxidative degradation. This approach is useful for degrading colored contaminants, e.g., textile dyes. This process of self-sensitized oxidation is particularly effective in degradation of colored pollutants with visible light. The key advantage is its inherent destructive nature: it does not involve mass transfer; it can be carried out under ambient conditions (atmospheric oxygen is used as oxidant) and may lead to complete mineralization of organic carbon into CO_2. Moreover, TiO_2 photocatalyst is largely available, inexpensive, non-toxic, and shows relatively high chemical stability.

Finally, TiO_2 photocatalytic process is receiving increasing attention due to its low cost when sunlight is employed as the irradiation source. The utilization of combined photocatalysis and solar technologies may develop a useful process for the reduction of water pollution by dying compounds, because of the mild conditions required and their efficiency in the mineralization.

The chemical classes of dyes that are employed more frequently on industrial scale are the azo, anthraquinone, sulfur, indigoid, triphenylmethyl (trityl), and phthalocyanine derivatives. However, it has to be emphasized that the overwhelming majority of synthetic dyes currently used in the industry are azo derivatives. Of the dyes available on the market today, approximately 50–70% are azo compounds, followed by the anthraquinone group. Azo dyes can be divided into monoazo, diazo, and triazo classes according to the presence of one or more azo bonds (–N=N–) and are found in various categories, i.e., acidic, basic, direct, disperse, and azoic pigments. Konstantinou and Albanis (2004) summarized azo dyes that were photocatalytically degraded with TiO_2. Some azo dyes and their dye precursors have been shown to be or are suspected to be human carcinogens as they form toxic aromatic amines. Therefore azo dyes are pollutants of high environmental impact, and were selected as the most relevant group of dyes concerning their degradation using TiO_2-assisted photocatalysis. It should be noted that azoketo hydrazone equilibria can be a vital factor in the easy breakdown of many of the azo dye system.

Acid orange 7, a representative of the class azo dyes, is the most studied compound among the azo dyes as far as its photocatalytic degradation under several experimental conditions is concerned. The dye acid orange 7 shows azo–hydrazone tautomerism. The hydrazone form of the dye shows a bathochromic shift in the absorption spectra ($\lambda_{max} = 485$ nm) whereas a shoulder at 430 nm is attributed to the azo form of the dye. The azo peak at 430 nm was observed only in the aqueous phase, in which the TiO_2 particles were suspended in a homogeneous solution of the azo dye (see Fig. 17) (Chatterjee and Dasgupta 2005). The hydrazone form of the dye was reportedly found to be more stable when adsorbed on the surface of the TiO_2 semiconductor. When the spectra of the dye adsorbed on the TiO_2 surface were observed in a dry phase, the absorption peak corresponding to the hydrazone form of the dye was seen at 485 nm but the peak at $\lambda = 430$ nm (corresponding to the azo) disappeared. However, a tail in the red region of the visible spectrum up to $\lambda = 600$ nm was reportedly observed. Also, a peak at $\lambda = 520$ nm was seen, which indicated the formation of a donor–acceptor complex between the dye and the semiconductor on the surface of the TiO_2 semiconductor. The dye was subjected to FT-IR spectroscopy to probe the chemical reactions occurring on the semiconductor surface at intervals of $t = 0$, 40, and 350 min. Results revealed the formation of many degradation products as the irradiation time proceeded from $t = 0$ to 350 min, due to the formation of new peaks and subjugation of old peaks with time. However, the absorption spectrum (recorded in solid state) of the dye taken after a 3-h irradiation of the TiO_2 suspension revealed no peaks corresponding to the two forms of the dye, indicating that the dye was effectively degraded (Bauer et al. 2001). The degradation pathways and the formation of by-products are also fully described (see Fig. 18) (Konstantinou and Albanis 2004). After the photoinjection of an electron in the conduction band of TiO_2, the cation

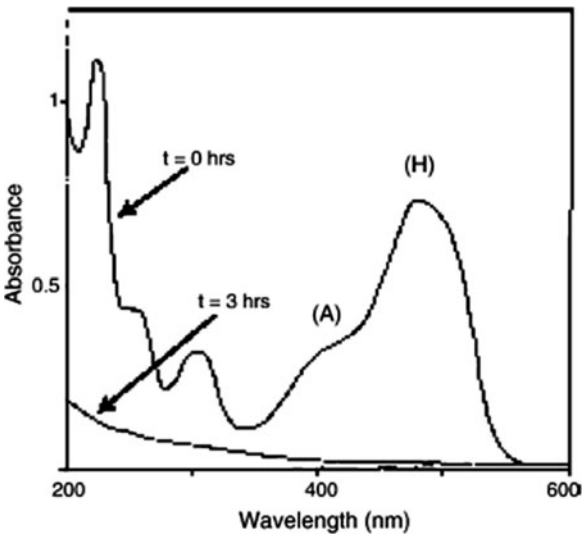

Fig. 17 Electronic absorption spectra of the aqueous solution ofAO7 at $t = 0$ h and after 3 h of irradiation with visible light beam ($\lambda = 442$ nm). H and A show the electronic absorption bands linked to the hydrazone and the azo tautomer, respectively. Reprinted from Chatterjee and Dasgupta (2005), Copyright with permission from Elsevier

radical formed from the hydrazone form of the dye can undergo rapid deprotonation to create the deprotonated radical, which can react with the molecular oxygen. This oxidative attack could lead to the formation of benzene sulfonate and napthaquinone but since napthaquinone is very unstable, it would further degenerate to form phthalic acid. Twenty-two transformation products were identified in total, including 2-naphthol, 2-hydroxy-1,4-naphthoquinone, smaller aromatic intermediates such as phthalic acid and phthalimide, and aliphatic acids such as fumaric, succinic, maleic, and malonic acids. The lowest molecular weight compounds detected were oxalic, acetic, and formic acids. Evidences in favor of the formation of several aliphatic carboxylic acids and oxygenated sulfur derivatives have been provided in the destruction of phthalic acid as well as benzene sulfonate. Though the photocatalytic formation of several active oxygen species via hydrogen peroxide, perhydroxyl, and hydroxyl radicals has been proposed for the degradation of the azo dyes, the role of these radicals has not yet been fully elucidated. It is possible that just neutral molecular oxygen or superoxide anions are sufficient for the degradation of the acid orange 7 dye (Bauer et al. 2001).

Acid orange 52, also known as methyl orange, is frequently selected from the aminoazobenzene sub-category of monoazo dyes. Up to 18 intermediates were identified including aniline, *N*,*N*-dimethyl aniline, hydroxy anilines, hydroxy analogues of acid orange 52, phenols, quinone, benzene sulphonic acid, demethylated analogues of acid orange 52, and various aliphatic and carboxylic acids. Spadaro et al. (1994) proposed that oxidation of aminoazobenzene dyes proceeds by the addition of a hydroxyl radical to the carbon atom bearing the azo bond, followed by

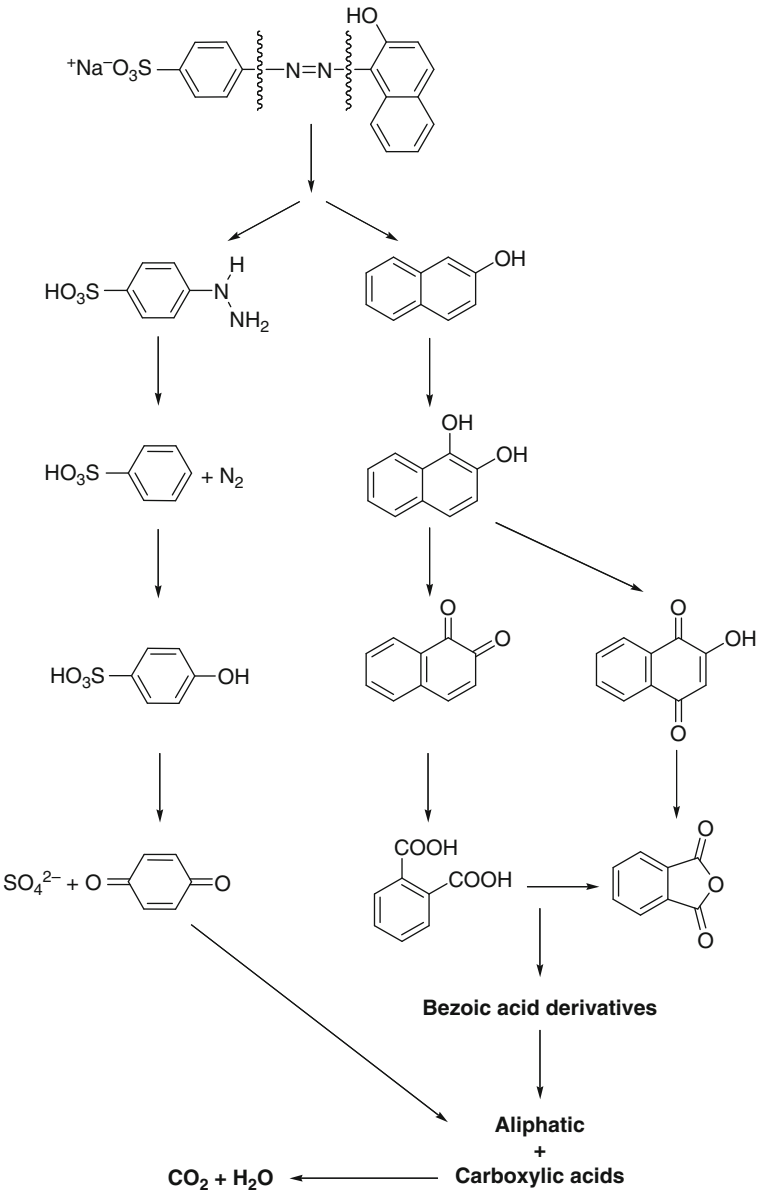

Fig. 18 Major photocatalytic pathways of acid orange 7. Reprinted from Konstantinou and Albanis (2004), Copyright with permission from Elsevier

the breaking of the resulting adduct. The products such as benzenesulfonic acid, *N*, *N*-dimethylaniline, and 4-hydroxy-*N*,*N*-dimethylaniline could arise from such reactions. The electron-withdrawing sulphonate group inhibits reactivity towards •OH of the ring that carried it, thus the ring with the amino group becomes the first target

for the hydroxy radicals. The addition of •OH on the carbon atom bearing the sulphonate group and the subsequent elimination of SO_3 is an improbable pathway due to the electron-withdrawing effect of sulphonate group and steric hindrance. On the contrary, hydroxyl-analogue derivatives of acid orange 52 are identified. The major degradation pathways for aminoazobenzene dyes are shown in Fig. 19 (Konstantinou and Albanis 2004).

Zhao et al. (2003) examined the effect of a TiO_2 surface-chemisorbed platinum (IV) chloride species ($PtCl_6^{2-}$) on the photodegradation of ethyl orange under visible light irradiation. Ethyl orange is an important representative of the azo dyes and is famous for its relatively stable features as a dye laser material. Addition of small quantities of hexachloroplatinic acid ($H_2PtCl_6{\cdot}6H_2O$) to the aqueous ethyl orange / TiO_2 dispersions significantly enhanced the degradation of the ethyl orange dye. Results also showed that $PtCl_6^{2-}$ was strongly adsorbed on the TiO_2 surface. In contrast, photodegradation appeared to be rather less efficient when carried out in the presence of TiO_2 alone. The primary step in the rapid degradation of the azo dye ethyl orange in the presence of $PtCl_6^{2-}$ is essentially the photoexcitation of the dye, not the excitation of adsorbed $PtCl_6^{2-}$, although the catalyst specimen does exhibit a definite light absorption throughout a portion of the visible wavelengths. As evidenced from the TOC and COD results, no intrinsic differences were observed between Pt(IV)/TiO_2 and TiO_2 dispersions in the mineralization of ethyl orange. It was emphasized that the existence of $PtCl_6^{2-}$ had a negligible effect on the mineralization of the substrate when the dispersion had been discolored. The discolored dispersions contain small molecular intermediates that have no absorption features in the visible region and thus cannot be excited by visible light. Accordingly, if localized excitation of $PtCl_6^{2-}$ were the primary step in the overall pathway, it should have led to the complete degradation (i.e., mineralization) of the azo dye. Proposed mechanism for the photodegradation of ethyl orange on Pt(IV)/TiO_2 surfaces is shown in Fig. 20 (Zhao et al. 2003).

6.2 *Nitroaromatic Compounds*

Environmental contamination by nitro compounds is associated principally with the xplosives industry. Modern explosives are nitrogen-containing organic compounds with the potential of self-oxidizing into small gaseous molecules (N_2, H_2O, and CO_2). Many are polynitroaromatic compounds, including 2,4,6-trinitrotoluene (TNT), (which for many years dominated the explosive industry), 1,3,5-trinitrobenzenene, dinitrotoluene (2,4-DNT, 2,6-DNT), dinitrobenzene, methyl-*N*,2,4,6-tetranitroaniline, and 2,4,6-trinitrophenol (picric acid). Some have additional industrial uses, e.g., the dinitrotoluenes are intermediates in the manufacture of polyurethanes.

Environmental contamination by nitro compounds is a problem because of the scale on which explosives have been manufactured, used, and tested. The United States ceased TNT production in the mid-1980s, but environmental contamination still exists due to activities before then and as a result of demilitarization.

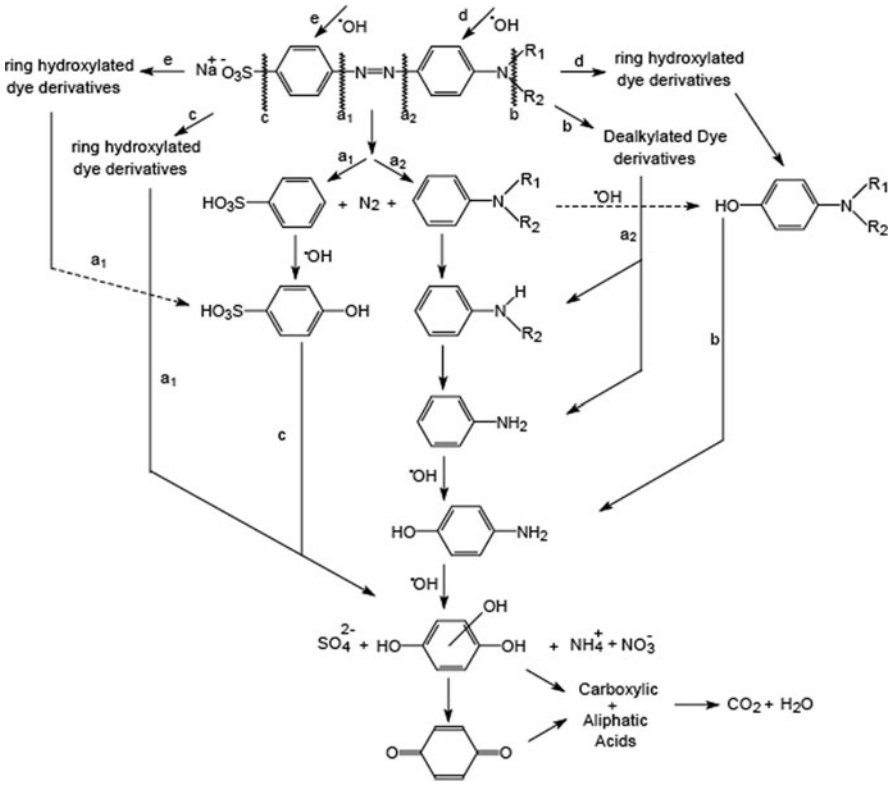

Fig. 19 Major photocatalytic degradation pathways for aminoazobenzene dyes based on the identification of by-products from degradation studies of acid orange 52. Reprinted from Konstantinou and Albanis (2004), Copyright with permission from Elsevier

Contamination occurs during the manufacture of TNT, which requires large amounts of water for purification. The aqueous wastes known as red water contains up to 30 nitroaromatics besides TNT. In addition, pink water, which is generated during loading, packing or assembling munitions, often contains high concentrations of other nitroaromatic explosives.

Nitroaromatic explosives are toxic, and their environmental transformation products, including arylamines, arylhydroxylamines, and condensed products such as azoxy and azo compounds, are equally or more toxic when compared to their parent nitroaromatics. Aromatic amines and hydroxylamines are implicated as carcinogenic intermediates as a result of nitrenium ions formed by enzymatic oxidation. TNT is on the list of US EPA priority pollutants: it is a known mutagen and can cause pancytopenia as a result of bone marrow failure. Aromatic nitro compounds are resistant to chemical or biological oxidation and to hydrolysis because of the electron-withdrawing nitro groups.

Rodgers and Bunce reviewed a variety of treatment technologies that are available or under research to remediate the contaminants, which include TiO_2 photocatalysis,

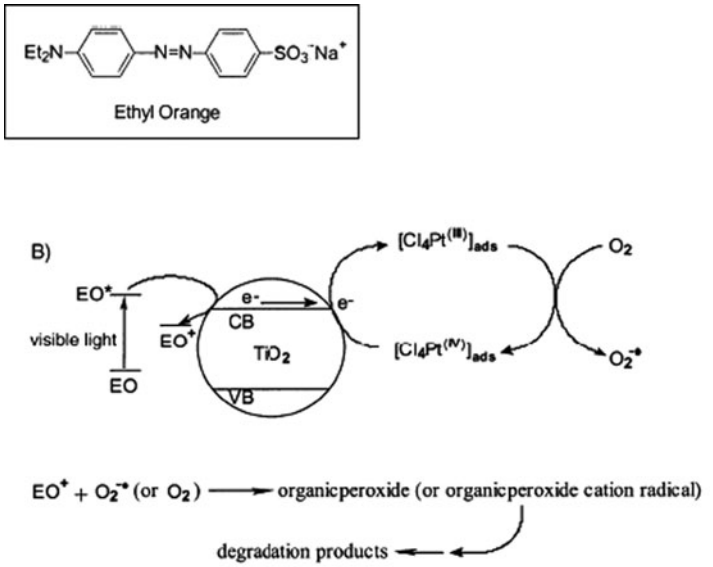

Fig. 20 Proposed mechanism for the photodegradation of ethyl orange on Pt(IV)/TiO_2 surfaces under irradiation with visible light where EO denotes ethyl orange the chemical structure of which is shown in a *square box* (Zhao et al. 2003)

UV oxidation with hydrogen peroxide, UV oxidation with ozone, Fe^{2+}/H_2O_2, Fe^{2+}/H_2O_2/UV, adsorption, surfactant complexing, liquid–liquid extraction, ultrafiltration, reverse osmosis, chemical reduction (hydrogenation), microorganism remediation, and phyto-remediation (Rodgers and Bunce 2001).

Heterogeneous photocatalysis is inefficient due to electron–hole recombination, which competes with water oxidation. However, the process has attracted much attention because it employs UVA radiation, wavelength of which ranges from 320 to 400 nm, that allows the use of low-cost near-UV lamps or even natural sunlight (although the latter has never been commercialized) and hinders the competing light absorption by other substances. In the aqueous slurry of TNT with TiO_2, the nitrogen atoms of TNT were converted to NH^{4+} and NO_3^- (Rodgers and Bunce 2001).

Kamble et al. (2006) studied the photocatalytic degradation of *m*-dinitrobenzene (*m*-DNB) by illuminated TiO_2 in a slurry reactor. *m*-DNB is one of the several compounds that are released to the environment during the manufacture of explosives and in loading, assembly and packing activities at military ammunition plants and other military installations. *m*-DNB is manufactured as a byproduct of the explosive TNT, with the potential for release to the environment in discharged wastewater. Additionally, any 2,4-dinitrotoluene present in the waste stream may be degraded to *m*-DNB by photolysis under certain pH conditions and organic matter content. Its widespread distribution as an environmental contaminant is a potential threat to wildlife and other ecological receptors. Therefore, removal of *m*-DNB from aqueous solution is very important. 2,4-Dinitrophenol and

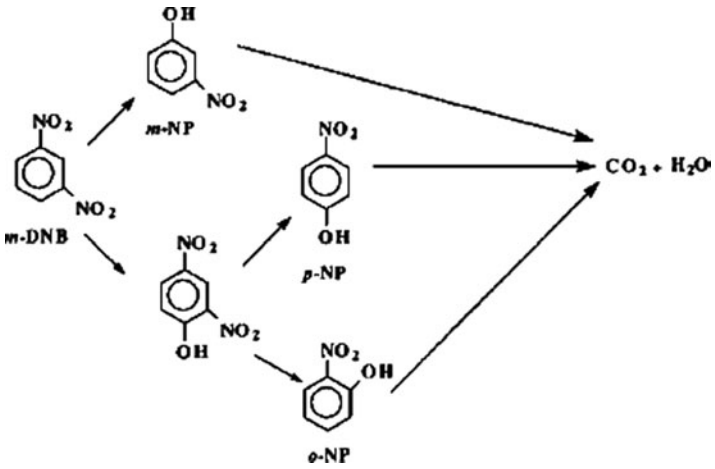

Fig. 21 Postulated reaction pathway for photocatalytic degradation of *m*-DNB where *o*-NP, *m*-NP, and *p*-NP denote *o*-nitrophenol, *m*-nitrophenol, and *p*-nitrophenol, respectively (Kamble et al. 2006)

m-, *o*-, and *p*-nitrophenol were detected as intermediates in very low concentrations during the degradation of *m*-DNB, using concentrated solar radiation and O_2 from air as the electron acceptor. It was observed that the rate of photocatalytic degradation of *m*-DNB is relatively low compared to that of nitrobenzene as a result of the poor adsorption of *m*-DNB compared to nitrobenzene. Figure 21 shows the postulated pathway for the photocatalytic decomposition of *m*-DNB.

7 Nitrogen-Containing Inorganic Compounds

In addition to organic compounds, a wide variety of inorganic compounds are photocatalytically sensitive on the surfaces of semiconductor particles. Toxic heavy metal ions can be reduced and deposited for easy disposal, since metal deposits can subsequently be extracted from the slurry by mechanical and/or chemical methods. The development of industries significantly increases the demand for metals. Waste metal recovery can potentially resolve two issues: metal pollution prevention and resource conservation. Metal ions are generally non-degradable, build up concentrations in food chains to toxic levels, and have infinite lifetimes. Hg^{2+}, Pb^{2+}, Cd^{2+}, Ag^{+}, Ni^{2+}, and Cr^{6+} ions that are well known for high toxicity are extracted by semiconductor-assisted photoreduction or deposited on the semiconductor as insoluble oxides, depending on relative positions of their redox potentials. Concentrations lower than 0.005 ppm are allowed for Cr^{6+} and Ni^{2+}, 0.004 ppm for Pb^{2+}, and 0.001 ppm for Hg^{2+}. The recommended level of Cd^{2+} is less than 5 ppm, also being included in the priority list of US EPA. The toxic effect of Ag^{+} is not completely understood but it is known as an effective bactericide that can damage

biological systems. Precious metals such as platinum, palladium, rhodium, gold, and copper can also be extracted by heterogeneous photodeposition.

In heterogeneous photocatalysis of organic substances, non-metal inorganic compounds are generated through subsequent total mineralization. The absence of total mineralization has been observed only in the case of *s*-triazine herbicides as mentioned earlier in this chapter. In this case, the final product obtained was essentially 2,4,6-trihydroxy-1,3,5-triazine (cyanuric acid), which is, fortunately, non-toxic. This is due to the high stability of the triazine nucleus, which resists most oxidation methods. For chlorinated molecules, Cl^- ions are easily released to the solution, which could be of interest in a process where photocatalysis is associated with a biological depuration system that is generally ineffective in treating chlorinated compounds. Sulfur-containing pollutants are mineralized into sulfate ions, whereas organophosphorous pesticides produce phosphate ions. However, phosphate ions remained adsorbed on TiO_2 within the pH range used. This strong adsorption partially lowers the reaction rate, which, however, remains acceptable. The analysis of aliphatic fragments resulting from the degradation of the aromatic ring has only revealed formate and acetate ions. Other aliphatics (presumably acids, diacids, and hydroxylated compounds) are very difficult to separate from water and to analyze. Formate and acetate ions are rather stable as observed in other advanced oxidation processes, which in part explain why the total mineralization takes much longer than dearomatization (Herrmann 1999).

Above all, ammonium (including ammonia), nitrate, and nitrite are the most frequently encountered and important inorganic species because nitrogen-containing organic molecules are mineralized into NH_4^+ and mostly NO_3^-. Ammonium ion is relatively stable and its proportion depends mainly on the initial oxidation degree of nitrogen and on the irradiation time. Presence of cyanide must not be overlooked because it is a significant source of the nitrogen-containing inorganic compounds.

The existence of free or complexed cyanides in industrial effluents is a problem of major concern because of infamous toxicity of these species to ecosystems. Cyanide has been used as an unparalleled leaching agent in the extraction of gold from ore. Harmful industrial aqueous wastes containing free or complexed cyanides are generated in large amounts from refining, electroplating, and heat-treating of gold as well as coal gasification process. There have been conventional treatment processes including physical, chemical, and biological methods to remove free or complexed cyanides dissolved in water. Physical treatments include ion exchange, adsorption by activated carbon, flotation-foam separation, reverse osmosis, and electrodialysis. Biological methods are based on biodegradation. Chemical processes involve the INCO process using SO_2-air, the Degussa process using hydrogen peroxide, electrolytic decomposition, cyanide oxidation by oxidants such as ferrate (VI), ozone, and permanganate, and alkaline chlorination, which is currently the most reliable technique. These methods, however, are not free from some drawbacks. For instance, in the physical treatments, cyanides are not decomposed or treated but only shifted from water to another phase. For biological methods, the reaction rate is so low that the method is limited to low concentrations of cyanides. For chemical processes, oxidants are generally expensive and some metal cyanide

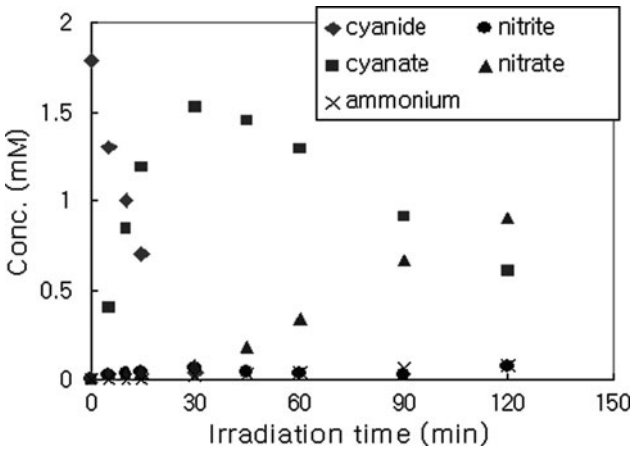

Fig. 22 Concentration of cyanide and products using TiO_2 when the suspension was bubbled with oxygen. Reprinted from Kim and Lee (2003), Copyright with permission from Elsevier

complexes are not decomposable by oxidation. Especially, for alkaline chlorination, highly toxic cyanogen chloride (CNCl) is produced (Kim and Lee 2004). Since the pioneer work by Frank and Bard, the photocatalytic decomposition of aqueous cyanide has been studied (Frank and Bard 1977; Kim et al. 2001; Chiang et al. 2002; Yeo et al. 2002; Sohn et al. 2003; Hernández-Alonso et al. 2002; Kim and Lee 2003). Cyanate reportedly appears as the first intermediate and undergoes further mineralization to ammonium, nitrite, nitrate, and gaseous products according to experimental conditions. Figure 22 shows the changes in the concentration of cyanide and the distribution of products using TiO_2 when the suspension was bubbled with oxygen (Kim 2003). It is still ambiguous whether the photocatalytic oxidation of cyanide proceeds via hydroxyl radicals or by photogenerated holes.

8 Application in Polymer Science

The active radical species such as hole or hydroxyl radicals originated from photocatalysis can be utilized to initiate polymerization or polymer decomposition according to reaction conditions. In the absence of water and oxygen, radicals can initiate polymerization. Styrene, 1,3,5,7-tetramethylcyclotetrasiloxane, methyl methacrylate, and pyrrole can be polymerized with photocatalysis (Fox and Duray 1993). When photocatalysts are incorporated into polymer matrices or coated on substrates, photocatalysis decomposes polymer matrices or polymeric substrates/binders, causing so-called weathering or chalking. Recently, many studies have been related with these phenomena to endow polymer-base materials with the positive effects of photocatalysis, such as self-cleaning property, anti-bacterial property, and self-degradation property for eco-friendly material (Gesenhues 2000, 2001; Allen

et al. 2004; Penot et al. 2003; Lacoste et al. 2003; Cho and Choi 2001; Zan et al. 2004; Xu et al. 2005; Kim et al. 2006; Sun et al. 2002; Iketania et al. 2003; Sanchez et al. 2006; Moustaghfir et al. 2006; Yang et al. 2006; Schmidt et al. 2006; Wakamura et al. 2003; Yoshida et al. 2006).

8.1 Photocatalyst as a Pigment

TiO_2, a representative photocatalyst, has been widely used as a white pigment for thermoplastic materials. However, its high photocatalytic activity can cause photo-degradation of thermoplastic materials. Therefore, commercial TiO_2 pigments must have a variety of properties: different crystal structures and surface modifications. Inorganic surface modification is needed to lower the activity of photocatalysts and additional organic surface modification is required to enhance the dispersibility of photocatalysts in polymer matrix. When PVC is pigmented with TiO_2, the weathering is affected by the type of TiO_2 pigment. Rutile TiO_2 pigment shows lower weathering rates than anatase TiO_2 due to its lower photocatalytic activity and Al-doping on rutile TiO_2 lowers photocatalytic activity to the level of commercially available white pigments (Gesenhues 2000). Therefore, Al_2O_3-doped rutile TiO_2 has been used as commercial whiter pigments. The weathering or chalking phenomenon of alkyd paint film containing TiO_2 pigments is also suppressed by Al-doping on TiO_2 pigments. It was reported that Al_2O_3 existing in bulk phase TiO_2 is functionally more important than surface Al_2O_3 because bulk Al_2O_3 provides recombination sites for hole and electrons (Gesenhues 2001). Besides Al_2O_3, SiO_2 can be coated on TiO_2 particles to inhibit the destructive oxidation of alkyd-based binders that leads to chalking phenomena. When hydrous aluminum oxide is used with other oxide materials, it decreases van der Waals force, which in turn improves the dispersibility. Particle size is also an important factor in determining the photo-oxidation rate of polyethylene. Nano-sized TiO_2 pigment showed higher photocatalytic activity in polyethylene degradation (Allen et al. 2004). For self-cleaning paint, it was suggested that a mixture of micron-sized rutile TiO_2 pigment with Al-doping and nano-sized anatase TiO_2 can be applied to limit the oxidation and chalking phenomena within the near surface layers (Allen et al. 2004). This application is dealt with as below.

ZnO also initiates the photocatalytic oxidations of isotactic propylene and ethylene–propylene copolymers in the absence of anti-oxidants or surface-coated layers (Penot et al. 2003; Lacoste et al. 2003).

8.2 Photocatalyst–Polymer Composite

In pigment/polymer system, photocatalytic oxidation has been an undesirable phenomenon to prevent. However, this reaction can be used in eco-friendly disposal of polymer wastes. Recently, photocatalyst–polymer composites have been

studied as self-degradable materials, decomposing under solar light via solid-phase photocatalysis.

When TiO_2 is embedded in polyvinylchloride (PVC), it is observed that PVC is photocatalytically degraded to a third of its molar weight after a 300-h irradiation. This phenomenon also takes place in the presence of oxygen, and cavity formation near TiO_2 aggregates is shown in Fig. 23. It seems that this degradation progressed via typical photocatalytic oxidation mechanism. However, the dispersion of TiO_2 was inefficient in PVC matrix, and it is suggested that only 0.02 wt% of TiO_2 is sufficient in decomposing PVC composite film when 5 nm TiO_2 particles are highly dispersed (Cho et al. 2001).

The dispersion of TiO_2 in polymer matrix can be enhanced by surface treatment. It was reported that polystyrene-grafted TiO_2 was prepared by the radical polymerization of polystyrene, following the pre-reaction of silicone coupling agent (γ-methacryloyloxypropyl triethoxysilane) and surface hydroxyl group of TiO_2. The grafted TiO_2 could be composited with polystyrene (PS) via radical polymerization, and showed higher dispersion and photocatalytic degradation efficiency in TiO_2-PS composite form than in unmodified TiO_2 form (see Fig. 24). The decomposition of TiO_2-PS composite was observed as in Fig. 25. After irradiating for 300-h, the average molecule weight of PS-grafted TiO_2 composite decreased to about a quarter of its original value (Zan et al. 2004). This composite can be applied for the accelerated natural degradation of PS and EPS (expanded polystyrene) packaging wastes.

Similarly, optically transparent poly(methyl methacrylate-*co*-maleic anhydride)/SiO_2–TiO_2 composite film can be prepared by using 3-aminopropyl triethoxysilane as a coupling agent to form imide groups. The composite film shows high thermal stability and photocatalytic degradation property (Xu et al. 2005).

TiO_2 can be surface-modified by hyperbranched poly(ε-caprolactone) (HPCL) with –COOH functional end groups. It was reported that HPCL-surface modification also enhanced the dispersibility of photocatalytic-degrading TiO_2 in PVC matrix (Kim et al. 2006).

HF surface-treatment of TiO_2 can increase the adsorption ability of TiO_2. HF-treated TiO_2 was mixed with PVC to make TiO_2-PVC composite film, and the enhanced adsorption property imparted by this incorporation reduced the emission of harmful chemicals such as dioxin. Harmful chemicals can be decomposed completely by subsequent photocatalysis (Sun et al. 2002).

8.3 Functional Coating on Polymeric Substrate

In recent years, photocatalysis has been applied to the coating technology. Surface coating with photocatalysts endows special properties to substrates as listed:

1. Hydrophilicity–hydrophobicity control
2. Self-cleaning property
3. Anti-bacterial property

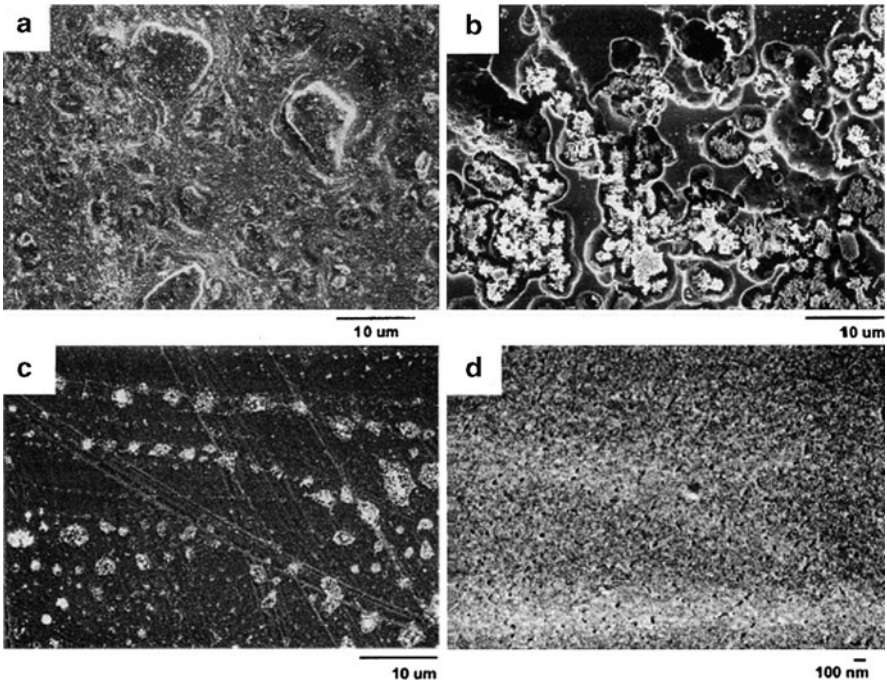

Fig. 23 SEM images of the pure PVC or PVC–TiO_2 (1.5 wt%) composite films: (**a**) PVC–TiO_2 film before irradiation; (**b**) PVC–TiO_2 film, 100-h irradiated; (**c**) PVC–TiO_2 film, 100-h irradiated under N_2; and (**d**) pure PVC film, 100-h irradiated (Cho et al. 2001). Reprinted from Cho and Choi (2001), Copyright with permission from Elsevier

4. UV-screening function

TiO_2 photocatalyst coating has been generally adapted on inorganic substrates. However, the coating on polymeric substrates is more attractive for practical applications. A well-known problem of photocatalyst coating on polymeric substrates is the degradation of substrates or binders by photocatalysis. To solve this problem, a special intermediate layer can be located between the photocatalyst coating layer and the substrate layer (Iketania et al. 2003). Additionally, an intermediate layer relaxes the stress exerted by the thermal expansion difference between the photocatalyst layer and the substrate layer. As an intermediate layer, inorganic/organic/hybrid (multi)layers can be used.

SiO_2 and Al_2O_3 are good candidates for inorganic intermediates. But, it is possible for inorganic intermediate layers to adhere poorly on polymeric substrates. When PET monolith was used as a TiO_2 photocatalyst support, SiO_2 intermediate layer was employed. To improve adherence, the surface of SiO_2 was coated with fluorinated surfactant to lower surface tension, or the surface of PET was modified

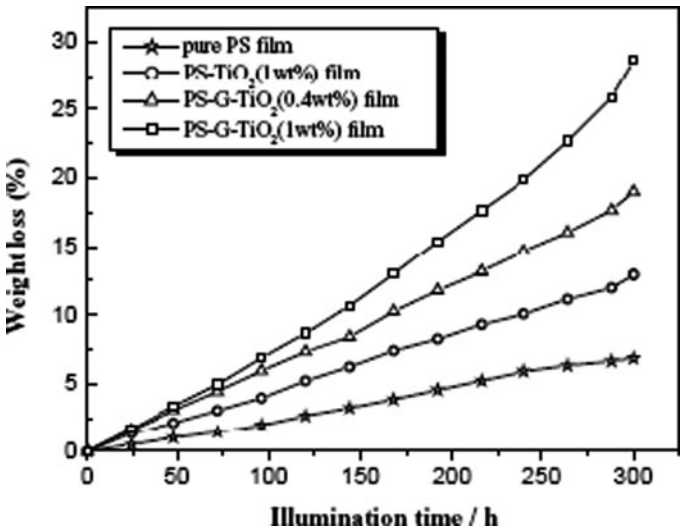

Fig. 24 Weight loss curve of pure PS, PS–TiO_2, and PS-grafted TiO_2 composite films under UV illumination in air. Reprinted from Zan et al. (2004), Copyright with permission from Elsevier

with a layer of poly(diallyldimethylammonium) chloride (PDDA) to form a positively charged surface (Sanchez et al. 2006).

The UV stability of polycarbonate (PC) film can be enhanced by ZnO coating. However, ZnO also results in photocatalytic oxidation of PC film and the effect of UV screening deteriorates. When Al_2O_3 interlayer was introduced between ZnO and PC layers by sputtering, UV stability of ZnO/PC film was enhanced due to the barrier effect of Al_2O_3 to O_2 (Moustaghfir et al. 2006).

Organic intermediate layer shows good adhesion property but poor affinity with the photocatalyst layer, and demonstrates long-term sustainability due to slow self-degradation. Therefore, organic–inorganic hybrid-multilayers are preferred as intermediate layers to prevent substrate degradation in practice. However, the coating procedure is so complicated that simple techniques excluding intermediate layers have been introduced.

When TiO_2/poly(dimethylsiloxane) (PDMS) hybrid sol was prepared through the sol–gel synthesis of TiO_2 in the presence of PDMS and spin-coated directly on poly(methylmethacrylate) (PMMA), the photocatalytic activity and stability of PMMA substrate were affected according to PDMS content as shown in Fig. 26 (Iketania et al. 2003). It seems that PDMS, at optimum amounts, enhances the affinity with PMMA substrate and suppresses the photocatalytic degradation of the substrate, sustaining the photocatalytic activity on organic compounds.

Also, the interfacial adherence between TiO_2 photocatalyst and acrylonitrile–butadiene–styrene polymer (ABS) could be enhanced without any interfacial layers, as TiO_2 was prepared in the presence of acetylacetone (Yang et al. 2006).

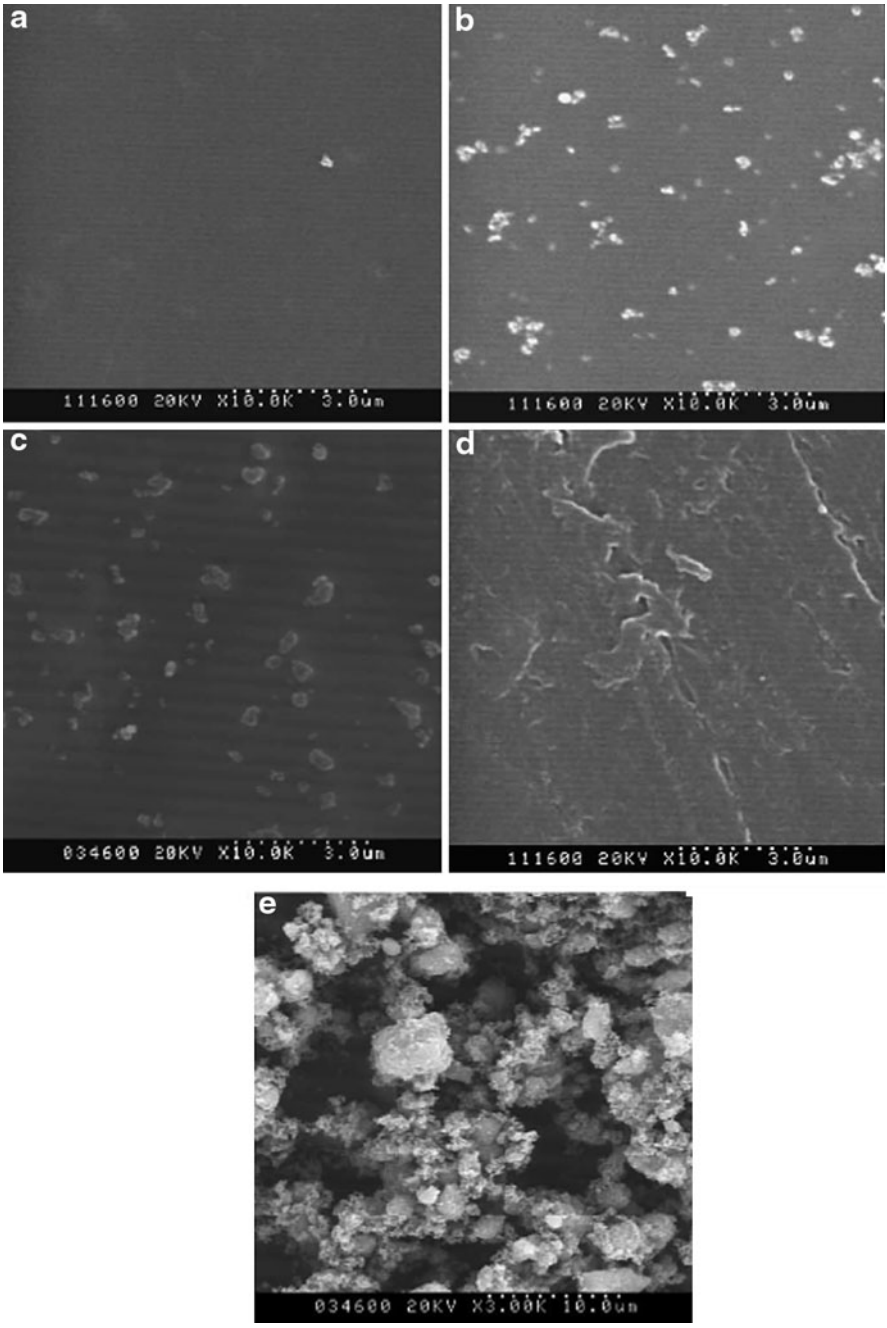

Fig. 25 SEM images of composite films: (**a**) pure PS film before irradiation, (**b**) PS–G-TiO_2 (1.0 wt%) film before irradiation, (**c**) PS–TiO_2 (1.0 wt%) composite film before irradiation, (**d**) pure PS film illuminated for 300-h, and (**e**) PS–G-TiO_2 (1.0 wt%) composite film illuminated for 300-h, Reprinted from Zan et al. (2004), Copyright with permission from Elsevier

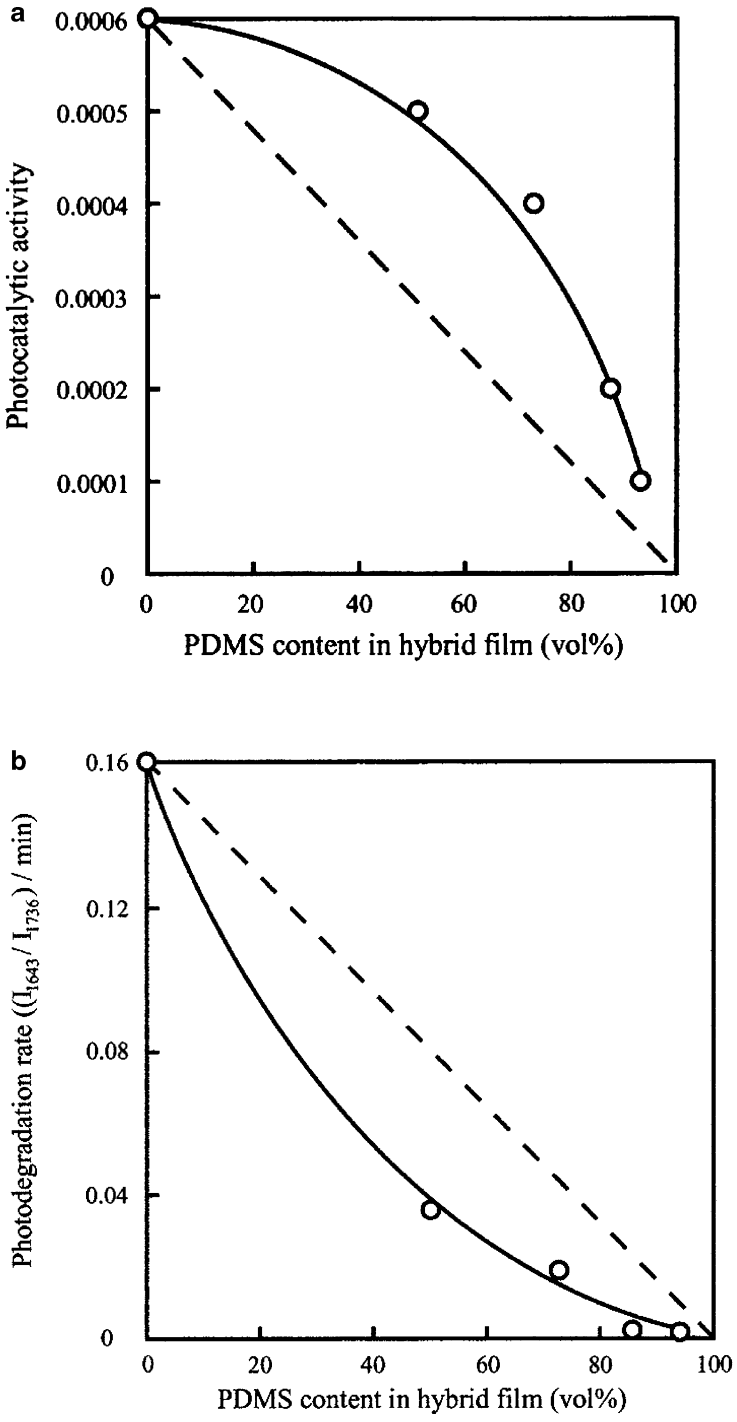

Fig. 26 Photodegradation rate for methylene blue (**a**) and of PMMA substrate (**b**) as a function of PDMS (vol%) in hybrid films. Reprinted from Iketania et al. (2003), Copyright with permission from Elsevier

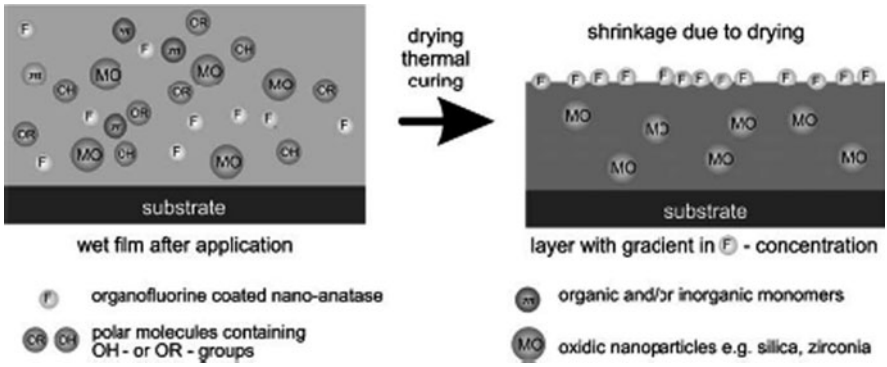

Fig. 27 Proposed mechanism of the gradient formation (Schmidt et al. 2006). Reprinted from Schmidt et al. (2006), Copyright with permission from Elsevier

Recently, photocatalyst gradient coating technology has been introduced (Schmidt et al. 2006). The surface of nano-size TiO_2 is modified with 3,3,4,4,5,5,6,6,7,7,8,8,8-tridecafluorooctyl-1,1,1-triethoxysilane (FTS) and mixed with methyltriehoxysilane (MTEOS), tetraethoxysilane (TEOS) sol, and binders such as NANOMER. The resulting mixture is coated on pre-treated PVC using primers. As the solvent is dried, a self-organizing gradient layer formation takes place with an up-concentration of photocatalyst at the interface layer between the coating and the air (see Fig. 27). After the activation by UV irradiation, the film shows good photocatalytic activities in pollutant-degrading, self-cleaning, and anti-fogging behaviors.

Calcium hydroxyapatite ($Ca_{10}(PO_4)_6(OH)_2$) doped with Ti^{4+} (TiHAP) shows photocatalytic activity in acetaldehyde and albumin decompositions (Wakamura et al. 2003). This material was applied with PMMA polymer binder to a special coating for photocatalytic self-cleaning effect and retained its photocatalytic activity due to highly stabilizing polymer binders. FAS treatment on TiHAP enhanced the stability of PMMA binder (Yoshida et al. 2006).

Although several approaches have been successfully tested to suppress the chalking or weathering behavior of polymer binders or substrates, many interests and studies are still needed for practical industrial applications of the photocatalyst.

References

Agustina TE, Ang HM, Vareek VK (2005) A review of synergistic effect of photocatalysis and ozonation on wastewater treatment. J Photochem Photobiol C Photochem Rev 6:264–273

Allen NS, Edge M, Ortega A, Sandoval G, Liauw CM, Verran J, Stratton J, McIntyre RB (2004) Degradation and stabilisation of polymers and coatings: nano versus pigmentary titania particles. Polym Degrad Stabil 85:927–946

Amorisco A, Losito I, Palmisano F, Zambonin PG (2005) Photocatalytic degradation of the herbicide isoproturon: characterization of by-products by liquid chromatography with electrospray ionization tandem mass spectrometry. Rapid Commun Mass Spectrom 19:1507–1516

Amorisco A, Losito I, Carbonara T, Palmisano F, Zambonin PG (2006) Photocatalytic degradation of phenyl-urea herbicides chlortoluron and chloroxuron: characterization of the by-products by liquid chromatography coupled to electrospray ionization tandem mass spectrometry. Rapid Commun Mass Spectrom 20:1569–1576

Andreozzi R, Caprio V, Insola A, Longo G, Tufano V (2000) Photocatalytic oxidation of 4-nitrophenol in aqueous TiO_2 slurries: an experimental validation of literature kinetic models. J Chem Technol Biotechnol 75:131–136

Anpo M, Shima T, Kodama S, Kubokawa Y (1987) Photocatalytic hydrogenation of CH_3CCH with H_2O on small-particle TiO_2: size quantization effects and reaction intermediates. J Phys Chem 91:4305–4310

Antonaraki S, Androulaki E, Dimotikali D, Hiskia A, Papaconstantinou E (2002) Photolytic degradation of all chlorophenols with polyoxometallates and H_2O_2. J Photochem Photobiol A Chem 148:191–197

Bamwenda GR, Uesigi T, Abe Y, Sayama K, Arakawa H (2001) The photocatalytic oxidation of water to O_2 over pure CeO_2, WO_3, and TiO_2 using Fe^{3+} and Ce^{4+} as electron acceptors. Appl Catal A Gen 205:117–128

Bauer C, Jacques P, Kalt A (2001) Photooxidation of an azo dye induced by visible light incident on the surface of TiO_2. J Photochem Photobiol A Chem 140:87–92

Beltrán FJ, Rivas FJ, Gimeno O (2005) Comparison between photocatalytic ozonation and other oxidation processes for the removal of phenols from water. J Chem Technol Biotechnol 80:973–984

Benitez FJ, Beltrán-Heredia J, Acero JL, Rubio FJ (2000) Rate constants for the reactions of ozone with chlorophenols in aqueous solutions. J Hazard Mater B 79:271–285

Bhatkhande DS, Pangarkar VG, Beenackers AACM (2001) Photocatalytic degradation for environmental applications: a review. J Chem Technol Biotechnol 77:102–116

Blake DM (2001) Bibliography of work on the heterogeneous photocatalytic removal of hazardous compounds from water and air. National Renewable Energy Laboratory, Golden, CO

Boule P, Guyon C, Lemaire J (1982) Photochemistry and environment IV: photochemical behaviour of monochlorophenols in dilute aqueous solution. Chemosphere 11:1179–1188

Brown DJ, Mason SF (1962) The pyrimidine. Wiley, New York

Burgeth G, Kisch H (2002) Photocatalytic and photoelectrochemical properties of titania-chloroplatinate(IV). Coord Chem Rev 230:41–47

Calza P, Medana C, Baiocchi C, Pelizzetti E (2004) Photocatalytic transformations of aminopyrimidines on TiO_2 in aqueous solution. Appl Catal B Environ 52:267–274

Calza P, Medana C, Baiocchi C, Hidaka H, Pelizzetti E (2006) Light-induced transformation of alkylurea derivatives in aqueous TiO_2 dispersion. Chem Eur J 12:727–736

Carp O, Huisman CL, Reller A (2004) Photoinduced reactivity of titanium dioxide. Prog Solid State Chem 32:33–177

Chatterjee D, Dasgupta S (2005) Visible light induced photocatalytic degradation of organic pollutants. J Photochem Photobiol C Photochem Rev 6:186–205

Chiang K, Amal R, Tran T (2002) Photocatalytic degradation of cyanide using titanium dioxide modified with copper oxide. Adv Environ Res 6:471–485

Chiron S, Fernandes-Alba A, Rodriguez A, Garcia-Clavo E (2000) Pesticide chemical oxidation: state-of-the-art. Water Res 34:366–377

Cho S, Choi W (2001) Solid-phase photocatalytic degradation of PVC–TiO_2 polymer composites. J Photochem Photobiol A Chem 143:221–228

Cho Y, Choi W, Lee C-H, Hyeon T, Lee H-I (2001) Visible light-induced degradation of carbon tetrachloride on dye-sensitized TiO_2. Environ Sci Technol 35:966–970

Choi W, Termin A, Hoffmann MR (1994) The role of metal ion dopants in quantum-sized TiO_2: correlation between photoreactivity and charge carrier recombination dynamics. J Phys Chem 98:13669–13679

Czaplicka M (2006) Photo-degradation of chlorophenols in the aqueous solution. J Hazard Mater B 134:45–59

Devi LG, Krishnaiah GM (1999) Photocatalytic degradation of *p*-amino-azo-benzene and *p*-hydroxy-azo-benzene using various heat treated TiO_2 as the photocatalyst. J Photochem Photobiol A Chem 121:141–145

Dhananjeyan MR, Annapoorani R, Lakshmi S, Renganathan R (1996) An investigation on TiO_2-assisted photo-oxidation of thymine. J Photochem Photobiol A Chem 96:187–191

Dhananjeyan MR, Annapoorani R, Renganathan R (1997) A comparative study on the TiO_2 mediated photo-oxidation of uracil, thymine and 6-methyluracil. J Photochem Photobiol A Chem 109:147–153

Dhananjeyan MR, Kandavelu V, Renganathan R (2000a) An investigation of the effects of Cu^{2+} and heat treatment on TiO_2 photooxidation of certain pyrimidines. J Mol Catal A Chem 158:577–582

Dhananjeyan MR, Kandavelu V, Renganathan R (2000b) A study on the photocatalytic reactions of TiO_2 with certain pyrimidine bases: effects of dopants (Fe^{3+}) and calcination. J Mol Catal A Chem 151:217–223

Diebold U (2003) The surface science of titanium dioxide. Surf Sci Rep 48:53–229

Ding Z, Lu Q, Greenfield PF (2000) Role of the crystallite phase of TiO_2 in heterogeneous photocatalysis for phenol oxidation in water. J Phys Chem B 104:4815–4820

Forgacs E, Cserháti T, Oros G (2004) Removal of synthetic dyes from wastewaters. Environ Int 30:953–971

Fox MA, Duray MT (1993) Heterogeneous photocatalysis. Chem Rev 93:341–357

Frank SN, Bard AJ (1977) Heterogeneous photocatalytic oxidation of cyanide ion in aqueous solutions at TiO_2 powder. J Am Chem Soc 99:303–304

Fujishima A, Honda K (1972) Electrochemical photolysis of water at a semiconductor electrode. Nature 238:37–38

Fujishima A, Rao TN, Tryk D (2000) Titanium dioxide photocatalysis. J Photochem Photobiol C Photochem Rev 1:1–21

Gesenhues U (2000) Influence of titanium dioxide pigments on the photodegradation of poly(vinyl chloride). Polym Degrad Stab 68:185–196

Gesenhues U (2001) Al-doped TiO_2 pigments: influence of doping on the photocatalytic degradation of alkyd resins. J Photochem Photobiol A Chem 139:243–251

Gogate PR, Pandit AB (2004) A review of imperative technologies for wastewater treatment I: oxidation technologies at ambient conditions. Adv Environ Res 8:501–551

Halmann MM (1996) Photodegradation of water pollutants. CRC, Boca Raton, FL

Hernández-Alonso MD, Coronado JM, Maira AJ, Soria J, Loddo V, Augugliaro V (2002) Ozone enhanced activity of aqueous titanium dioxide suspensions for photocatalytic oxidation of free cyanide ions. Appl Catal B Environ 39:257–267

Herrmann J-M (1995) Heterogeneous photocatalysis: an emerging discipline involving multiphase systems. Catal Today 24:157–164

Herrmann J-M (1999) Heterogeneous photocatalysis: fundamentals and applications to the removal of various types of aqueous pollutants. Catal Today 53:115–129

Hirakawa T, Nokada Y (2002) Properties of $O_2^{\bullet -}$ and OH• formed in TiO_2 aqueous suspensions by photocatalytic reaction and the influence of H_2O_2 and some ions. Langmuir 18:3247–3254

Hoffmann MR, Martin ST, Choi W, Bahnemann DW (1995) Environmental applications of semiconductor photocatalysis. Chem Rev 95:69–96

Hofstadler K, Bauer R, Novalic S, Heisler G (1994) New reactor design for photocatalytic wastewater treatment with TiO_2 immobilized on fused-silica glass fibers: photomineralization of 4-chlorophenol. Environ Sci Technol 28:670–674

Hong S-S, Ju C-S, Lim C-G, Ahn B-H, Lim K-T, Lee G-D (2001) A photocatalytic degradation of phenol over TiO_2 prepared by sol–gel method. J Ind Eng Chem 7:99–104

Horikoshi S, Hidaka H (2001) Photodegradation mechanism of heterocyclic two-nitrogen containing compounds in aqueous TiO_2 dispersions by computer simulation. J Photochem Photobiol A Chem 141:201–208

Horikoshi S, Serpone N, Yoshizawa S, Knowland J, Hidaka H (1999) Photocatalyzed degradation of polymers in aqueous semiconductor suspensions. IV. Theoretical and experimental examination of the photooxidative mineralization of constituent bases in nucleic acids at titania/water interfaces. J Photochem Photobiol A Chem 120:63–74

Iketania K, Sun R-D, Toki M, Hirota K, Yamaguchi O (2003) Sol–gel-derived TiO_2/poly (dimethylsiloxane) hybrid films and their photocatalytic activities. J Phys Chem Solids 64:507–513

Jaussaud C, Pässe O, Faure R (2000) Photocatalysed degradation of uracil in aqueous titanium dioxide suspensions: mechanisms, pH and cadmium chloride effects. J Photochem Photobiol A Chem 130:157–162

Jung KS, Lee H-I (1997) Photocatalysis and its applications. J Korean Chem Soc 41:682–710

Jung KY, Park SB (1999) Anatase-phase titania: preparation by embedding silica and photocatalytic activity for the decomposition of trichloroethylene. J Photochem Photobiol A Chem 127:117–122

Kamble SP, Sawant SB, Pangarkar VG (2006) Photocatalytic degradation of *m*-dinitrobenzene by illuminated TiO_2 in a slurry photoreactor. J Chem Technol Biotechnol 81:365–373

Kim J-H (2003) Photocatalytic oxidation of aqueous cyanide using TiO_2 and heteropoly-tungstate-modified TiO_2. Ph.D. Thesis, Seoul National University, Seoul

Kim J-H, Lee H-I (2003) Activity of TiO_2 and heteropolytungstate-modified TiO_2 in the photocatalytic degradation of aqueous cyanide. Stud Surf Sci Catal 145:161–164

Kim J-H, Lee H-I (2004) Effect of surface hydroxyl groups of pure TiO_2 and modified TiO_2 on the photocatalytic oxidation of aqueous cyanide. Korean J Chem Eng 21:116–122

Kim H-J, Lu L, Kim J-H, Lee C-H, Hyeon T, Choi W, Lee H-I (2001) UV light induced photocatalytic degradation of cyanides in aqueous solution over modified TiO_2. Bull Korean Chem Soc 22:1371–1374

Kim SH, Kwak S-Y, Suzuki T (2006) Photocatalytic degradation of flexible PVC/TiO_2 nanohybrid as an eco-friendly alternative to the current waste landfill and dioxin-emitting incineration of post-use PVC. Polymer 47:3005–3016

Kiwi J (1985) Direct observation of the variation of energy levels in powdered TiO_2 as a function of temperature. Beneficial effects for energy conversion through semiconductor devices. J Phys Chem 89:2437–2439

Konstantinou IK, Albanis TA (2003) Photocatalytic transformation of pesticides in aqueous titanium dioxide suspensions using artificial and solar light: intermediates and degradation pathways. Appl Catal B Environ 42:319–335

Konstantinou IK, Albanis TA (2004) TiO_2-assisted photocatalytic degradation of azo dyes in aqueous solution: kinetic and mechanistic investigations. Appl Catal B Environ 49:1–14

Kormann C, Bahnemann DW, Hoffmann R (1988) Preparation and characterization of quantum-size titanium dioxide. J Phys Chem 92:5196–5201

Kouloumbos VN, Tsipi DF, Hiskia AE, Nikolic D, van Breemen RB (2003) Identification of photocatalytic degradation products of diazinon in TiO_2 aqueous suspensions using GC/MS/MS and LC/MS with quadrupole time-of-flight mass spectrometry. J Am Soc Mass Spectrom 14:803–817

Kuo WS (1999) Synergistic effects of combination of photolysis and ozonation on destruction of chlorophenols in water. Chemosphere 39:1853–1860

Lackhoff M, Prieto X, Nestle N, Dehn F, Niessner R (2003) Photocatalytic activity of semiconductor-modified cement: influence of semiconductor type and cement ageing. Appl Catal B Environ 43:205–216

Lacoste J, Singh RP, Boussand J, Arnaud R (2003) TiO_2-, ZnO-, and CdS-photocatalyzed oxidation of ethylene–propylene thermoplastic elastomers. J Polym Sci A Polym Chem 25:2799–2812

Lea J, Adesina AA (2001) Oxidative degradation of 4-nitrophenol in UV-illuminated titania suspension. J Chem Technol Biotechnol 76:803–810

Lee H-S (2004) Development of TiO_2 catalyst for the photocatalytic oxidation of 2-isopropyl-6-methyl-4-pyrimidinol. Ph.D. Thesis, Seoul National University, Seoul

Lee GD, Lee H-I (1992) Application of photocatalysis. J Korean Ind Eng Chem 3:35–45

Lee SG, Lee H-I (1998) A new sulfur-sensitive bismuth oxide on titania for photocatalyst. Korean J Chem Eng 15:463–468

Lee S-A, Choo K-H, Lee C-H, Lee H-I, Hyeon T, Choi W, Kwon H-H (2001a) Use of ultrafiltration membranes for the separation of TiO_2 photocatalysts in drinking water treatment. Ind Eng Chem Res 40:1712–1719

Lee SG, Kim J-H, Lee S, Lee H-I (2001b) Photochemical production of hydrogen from alkaline solution containing polysulfide dyes. Korean J Chem Eng 18:894–897

Lee SG, Lee S, Lee H-I (2001c) Photocatalytic production of hydrogen from aqueous solution containing CN^- as a hole scavenger. Appl Catal A Gen 207:173–181

Lee H-S, Hur T, Kim S, Kim J-H, Lee H-I (2003) Effects of pH and surface modification of TiO_2 with SiO_x on the photocatalytic degradation of a pyrimidine derivative. Catal Today 84:173–180

Lee H-S, Hur T, Kim S, Kim J-H, Lee H-I (2004) Influences of electron scavenger and conduction band position of photocatalyst on the degradation of a pyrimidine derivative. J Chem Eng Jpn 37:174–180

Lee H-S, Woo C-S, Youn B-K, Kim S-Y, Oh S-T, Sung Y-E, Lee H-I (2005) Bandgap modulation of TiO_2 and its effect on the activity in photocatalytic oxidation of 2-isopropyl-6-methyl-4-pyrimidinol. Top Catal 35:255–260

Lin J, Yu JC, Lo D, Lam SK (1999) Photocatalytic activity of rutile $Ti_{1-x}Sn_xO_2$ solid solutions. J Catal 183:368–372

López MC, Fernández MI, Rdgríguez S, Santaballa JA, Steenken S, Vulliet E (2005) Mechanisms of direct and TiO_2-photocatalysed UV degradation of phenylurea herbicides. ChemPhysChem 6:2064–2074

Malato S, Blanco J, Richter C, Maldonado MI (2000) Optimization of pre-industrial solar photocatalytic mineralization of commercial pesticides: application to pesticide container recycling. Appl Catal B Environ 25:31–38

Matthews RW (1987) Photooxidation of organic impurities in water using thin films of titanium dioxide. J Phys Chem 91:3328–3333

Mills G, Hoffmann R (1993) Photocatalytic degradation of pentachlorophenols on TiO_2 particles: identification of intermediates and mechanism of reaction. Environ Sci Technol 27:1681–1689

Mills A, Le Hunte S (1997) An overview of semiconductor photocatalysis. J Photochem Photobiol A Chem 108:1–35

Minero C, Pelizzetti E, Malato S, Blanco J (1996) Large solar plant photocatalytic water decontamination: degradation of atrazine. Sol Energy 56:411–419

Moustaghfir A, Tomasella E, Jacquet M, Rivaton A, Mailhot B, Gardette JL, Bêche E (2006) ZnO/Al_2O_3 coatings for the photoprotection of polycarbonate. Thin Solid Films 515:662–665

Moza PN, Fytianos K, Samanidou V, Korte F (1988) Photodecomposition of chlorophenols in aqueous medium in presence of hydrogen peroxide. Bull Environ Contam Toxicol 41:678–682

Nedoloujko A, Kiwi J (2000) TiO_2 speciation precluding mineralization of 4-tert-butylpyridine. Accelerated mineralization via Fenton photo-assisted reaction. Water Res 34:3277–3284

Oh S-T, Lu L, Lee H-I (2006) Intrinsic effect of H_2O on the structural characteristic of TiO_2 synthesized by using polyethylene glycol as template. Mater Lett 60:2795–2798

Oh S-T, Choi J-S, Lee H-S, Lu L, Kwon H-H, Song IK, Kim JJ, Lee H-I (2007) H_2O-controlled synthesis of TiO_2 with nanosized channel structure through in situ esterification and its application to photocatalytic oxidation. J Mol Catal A Chem 267:112–119

Ohno T, Sarukawa K, Matsumura M (2001) Photocatalytic activities of pure rutile particles isolated from TiO_2 powder by dissolving the anatase component in HF solution. J Phys Chem B 105:2417–2420

Ollis DF, Al-Ekabi H (1993) Photocatalytic purification and treatment of water and air. Elsevier, New York

Ozoemena K, Kuznetsova N, Nyokong T (2001) Comparative photosensitized transformation of polychlorophenols with different sulphonated metallophthalocyanine complexes in aqueous medium. J Mol Catal A Chem 176:29–40

Penot G, Arnaud R, Lemaire J (2003) ZnO-photocatalyzed oxidation of isotactic polypropylene. Angew Makromol Chem 117:71–84

Pirkanniemi K, Sillanpää M (2002) Heterogeneous water phase catalysis as an environmental application: a review. Chemosphere 48:1047–1060

Porter JF, Li Y-G, Chan CK (1999) The effect of calcination on the microstructural characteristics and photoreactivity of Degussa P-25 TiO_2. J Mater Sci 34:1523–1531

Ray AK, Beenackers AACM (1998) Development of a new photocatalytic reactor for water purification. Catal Today 40:73–83

Rodgers JD, Bunce NJ (2001) Treatment methods for the remediation of nitroaromatic explosives. Water Res 35:2101–2111

Sakthivel S, Kisch H (2003) Photocatalytic and photoelectrochemical properties of nitrogen-doped titanium dioxide. ChemPhysChem 4:487–490

Sanchez B, Coronado JM, Candal R, Portela R, Tejedor I, Anderson MA, Tompkins D, Lee T (2006) Preparation of TiO_2 coatings on PET monoliths for the photocatalytic elimination of trichloroethylene in the gas phase. Appl Catal B Environ 66:295–301

Schmidt H, Naumann M, Muller TS, Akarsu M (2006) Application of spray techniques for new photocatalytic gradient coatings on plastics. Thin Solid Films 502:132–137

Serpone N, Khairutdinov RF (1997) Application of nanoparticles in the photocatalytic degradation of water pollutants. Stud Surf Sci Catal 103:417–444

Serpone N, Lawless D, Khairutdinov R (1995) Size effects on the photophysical properties of colloidal anatase TiO_2 particles: size quantization versus direct transitions in this indirect semiconductor? J Phys Chem 99:16646–16654

Shen Y-S, Ku Y, Lee K-C (1995) The effect of light absorbance on the decomposition of chlorophenols by ultraviolet radiation and U.V./H_2O_2 processes. Water Res 29:907–914

Sohn D-R, Kim J-H, Lee S, Lee H-I (2003) The effect of H_2O_2 on the photodegradation of cyanide over TiO_2 catalyst. J Korean Ind Eng Chem 14:391–396

Spadaro JT, Isabelle L, Renganathan V (1994) Hydroxyl radical mediated degradation of azo dyes: evidence for benzene generation. Environ Sci Technol 28:1389–1393

Sun R-D, Nishikawa T, Nakajima A, Watanabe T, Hashimoto K (2002) TiO_2/polymer composite materials with reduced generation of toxic chemicals during and after combustion-effect of HF-treated TiO_2. Polym Degrad Stabil 78:479–484

Takeda N, Iwata N, Torimoto T, Yoneyama H (1998) Influence of carbon black as an adsorbent used in TiO_2 photocatalyst films on photodegradation behaviors of propyzamide. J Catal 177:240–246

Tratnyek PG, Holgné J (1991) Oxidation of substituted phenols in the environment: a QSAR analysis of rate constants for reaction with singlet oxygen. Environ Sci Technol 25:1596–1604

Turchi CS, Ollis DF (1990) Photocatalytic degradation of organic water contaminants: mechanisms involving hydroxyl radical attack. J Catal 122:178–192

Vulliet E, Emmelin C, Chovelon J-M, Guillard C, Herrmann J-M (2002) Photocatalytic degradation of sulfonylurea herbicides in aqueous TiO_2. Appl Catal B Environ 38:127–137

Wakamura M, Hashimoto K, Watanabe T (2003) Photocatalysis by calcium hydroxyapatite modified with Ti(IV): albumin decomposition and bactericidal effect. Langmuir 19:3428–3431

Wang K-H, Hsieh Y-H, Chou M-Y, Chang C-Y (1999) Photocatalytic degradation of 2-chloro and 2-nitrophenol by titanium dioxide suspensions in aqueous solution. Appl Catal B Environ 21:1–8

Xu J, Shi W, Gong M, Yu F, Yan L (2005) Preparation of poly(methyl methacrylate-*co*-maleic anhydride)/SiO_2–TiO_2 hybrid materials and their thermo- and photodegradation behaviors. J Polym Sci A Polym Chem 97:1714–1724

Yang J-H, Han Y-S, Choy J-H (2006) TiO_2 thin-films on polymer substrates and their photocatalytic activity. Thin Solid Films 495:266–271

Yawalkar AA, Bhatkhande DS, Pangarkar VG, Beenackers AACM (2001) Solar-assisted photochemical and photocatalytic degradation of phenol. J Chem Technol Biotechnol 76:363–370

Yeo S-W, Kim J-H, Lee H-I (2002) Photocatalytic treatment of cyanide in water. J Korean Chem Soc 46:64–68

Yoshida N, Takeuchi M, Okura T, Monma H, Wakamura M, Ohsaki H, Watanabe T (2006) Superhydrophobic photocatalytic coatings utilizing apatite-based photocatalyst. Thin Solid Films 502:108–111

Zan L, Tian L, Liu Z, Peng Z (2004) A new polystyrene-TiO_2 nanocomposite film and its photocatalytic degradation. Appl Catal A Gen 264:237–242

Zhao W, Chen C, Ma W, Zhao J, Wang D, Hidaka H, Serpone N (2003) Efficient photoinduced conversion of an azo dye on hexachloroplatinate(IV)-modified TiO_2 surfaces under visible light irradiation: a photosensitization pathway. Chem Eur J 9:3292–3299

Ziegmann M, Doll T, Frimmel FH (2006) Matrix effects on the photocatalytical degradation of dichloroacetic acid and atrazine in water. Acta Hydrochim Hydrobiol 34:146–154